



WPI

Design, Realization, and Application of a Positioner for High Resolution Optical Metrology in Aerostructures

A Major Qualifying Project

submitted to the Faculty of

WORCESTER POLYTECHNIC INSTITUTE

in partial fulfillment of the requirements for the

Degree of Bachelors of Science

By:

Paige Campagna and Ryan Powers

4/25/2024

Report Submitted to:

Prof. Cosme Furlong

This report represents the work of one or more WPI undergraduate students submitted to the faculty as evidence of completion of a degree requirement. WPI routinely publishes these reports on the web without editorial or peer review.

Abstract

Quantitative holography is an accepted technology used in the aerospace industry to quantify reliability and performance of structures prior to their deployment and use. Holography is capable of measuring static and dynamic deformations with nanometer resolution, enabling characterization of structural dynamics and defects. An existing holographic testing system for large samples relies on a fixed coordinate system, requiring the sample to be moved to different orientations using heavy machinery. This is costly and time consuming; therefore, there is a need for a more flexible approach to measure large samples. This project aims to develop a positioner capable of moving a holographic camera around a fixed sample while maintaining the mechanical stability required to obtain accurate optical measurements. The necessary degrees of freedom were identified, and a mechanism was chosen and modified through analytical computational and experimental methods. The resulting mechanism was applied to test components and demonstrate the required positioning and measuring capabilities.

Societal Impacts

This project aims to improve the safety of aerostructures using holographic testing. The success of this project helps to ensure the safety of passengers, crew, and pilots during flight by ensuring all components of the engine are suitable for use. Without such testing, the potential for accidents increases, posing heightened risks to all air travelers.

Table of Contents

Abstract.....	ii
Societal Impacts	iii
Table of Contents.....	iv
List of Figures.....	vi
List of Tables	vii
Acknowledgments	viii
Nomenclature.....	ix
Problem Statement.....	x
1.0 Introduction.....	1
2.0 Background.....	4
2.1 Basic Principles of Holography	4
2.2 Time-Averaged Method for Holographic Vibration Analysis.....	4
2.3 Positioners Used for Holography.....	5
3.0 Methodology.....	7
3.1 Methodology.....	7
3.2 Constraints and Functional Specifications.....	8
3.3 Positioner Selection	9
3.4 Computational Modeling	14
3.4.1 Detailed Design.....	14
3.4.2 Parametric Analyses	15
3.5 Experimental Validation and Testing	20
3.5.1 Impact Testing with Three Laser Doppler Vibrometers	20
3.5.2 Comparing the Magnitude of the First Natural Frequency of the Modified Positioner.....	29
3.5.3 Determining How Each DOF Impacts Stability of Optical Measurements.....	29
4.0 Results and Applications	32
5.0 Conclusions and Future Work	33
References.....	34
Appendices.....	35
Appendix 1: Gantt Chart of A, B, C, and D Term.....	35

Appendix 2: Constraints and Functional Specifications	37
Appendix 3: Static Analysis of Unmodified and Modified Positioner Mechanisms.....	41
Appendix 4: Dynamic Analysis of Unmodified and Modified Positioner Mechanisms	48
Appendix 5: LabVIEW Programs.....	56
Appendix 6: Test Conditions to Determine How Each DOF Impacts Stability of Optical Measurements	59

List of Figures

<i>Figure 1: Pratt & Whitney Boeing 747 SP (Boeing 747SP, 2024).....</i>	<i>1</i>
<i>Figure 2: Airplane Engine Fatigue (Pons, Aust, 2019).....</i>	<i>2</i>
<i>Figure 3: Schematic of Typical Holographic Setup</i>	<i>4</i>
<i>Figure 4: Holography Setup Used in CHSLT Lab at WPI. Positioner is Constrained Requiring the Movement of Sample Around Positioner. For Larger Components, it is Desirable to Keep Object Fixed and Move Holographic Camera Around Object for Inspection to Minimize Inspection Time and Cost.....</i>	<i>6</i>
<i>Figure 5: Flowchart of the Methodology Used in this Project.....</i>	<i>7</i>
<i>Figure 6: Kinematic Model of Mechanism with Required DOFs.....</i>	<i>10</i>
<i>Figure 7: Considered Mechanisms to Satisfy Necessary DOFs, Boom Stand (Scienscope, 2024), Balanced Four Bar (Edelkrone, 2024), and Articulating Arm (FX Articulating Arm, 2024)</i>	<i>10</i>
<i>Figure 8: Mechanism Integrated into Holographic Inspection System.....</i>	<i>12</i>
<i>Figure 9: Idealized Model of Selected Mechanism Including Mass Representing End Effector and Mass Representing Counterbalance Weights</i>	<i>13</i>
<i>Figure 10: Detailed SolidWorks Model of Unmodified Positioning System</i>	<i>14</i>
<i>Figure 11: Detailed SolidWorks Model of Modified Positioning System. Modifications Include a New Base of the Four Bar Mechanism (Highlighted in Red) and a New End Effector Connection (Highlighted in Blue) Obtained Through Analysis While Accounting for the Structural and Dynamic Characteristics of the Positioner to Minimize Structural Effects on the Holographic Measurements.</i>	<i>15</i>
<i>Figure 12: Safety Factor of the Unmodified Mechanism From 4.954 to over 100.</i>	<i>16</i>
<i>Figure 13: Safety Factor of the Modified Mechanism From 5.993 to over 100. This Shows an Increase in the Safety Factor Along the Extended Bars Holding the End Effector.....</i>	<i>17</i>
<i>Figure 14: Predicted the Shift of the Natural Frequencies After Structural Modifications. This Shows an Overall and Complex Increase in Natural Frequencies Post Modification While Maintaining Low Natural Frequencies When Compared to Sample.</i>	<i>19</i>
<i>Figure 15: Testing Setup with LDVs and Positioner.</i>	<i>20</i>
<i>Figure 16: Three LDV Lasers Aimed at the Optical Head in the X-, Y-, and Z- Directions.</i>	<i>21</i>
<i>Figure 17: Wiring Diagram of LDV Setup.</i>	<i>22</i>

<i>Figure 18: Visual Wiring Connections. NI Shown Top Left, LDVs Shown Top Right, Current Source Bottom Left and Impact Hammer Bottom Right.</i>	24
<i>Figure 19: MEMS Accelerometer (ADXL 326) Wiring Diagram.</i>	25
<i>Figure 20: MEMS Accelerometer (ADXL 326) Attached to the Polytec Stand.</i>	25
<i>Figure 21: Impact Hammer Next and Impact Zone in the X-Direction Marked in Red Tape.</i>	26
<i>Figure 22: Frequency Responses in the X-Direction.</i>	27
<i>Figure 23: Frequency Responses in the Y-Direction.</i>	28
<i>Figure 24: Frequency Responses in the Z-Direction.</i>	28
<i>Figure 25: The Setup for Holographic Testing a Representative Rotor Sample.</i>	30
<i>Figure 26: Stitched Holographic Image of a Commercial Avionics Rotor and Four Selected Individual Holographic Images.</i>	32

List of Tables

<i>Table 1: Example of a Constraint Taken from Appendix 2</i>	9
<i>Table 2: Requirements Satisfied by Boom Stand, Balanced Four Bar, and Articulating Arm.</i>	11
<i>Table 3: X-, Y-, Z-, and Resultant Component for Mode 1 of the Balanced Four bar Mechanism Before Modifications.</i>	18
<i>Table 4: X-, Y-, Z-, and Resultant Component for Mode 1 of the Balanced Four bar Mechanism with a Modified Base and End Effector. The Mode Shapes are Consistent Before and After Modification, With a Frequency Shift.</i>	19
<i>Table 5: List of Devices Used for Impact Hammer Testing.</i>	23
<i>Table 6: The Magnitude of the First Natural Frequency of the Modified Positioner Found Analytically, Computationally, and Experimentally.</i>	29

Acknowledgments

We would like to express our sincere gratitude to our project advisor, Professor Cosme Furlong-Vazquez, for his invaluable guidance and expertise throughout the project process. His insightful feedback was instrumental in shaping our project and navigating through challenges effectively.

We thank Daniel Ruiz-Cadalso, for his unwavering support, encouragement, and mentorship. His willingness to grant us access to his holographic system and share his expertise on holography propelled our project forward.

We extend our gratitude to the Center for Holographic Studies and Laser Micro Mechatronics (CHSLT) at Worcester Polytechnic Institute (WPI) for granting us access to their facilities where we completed most of our work. Special thanks are due to Howard Zheng, Anthony Salerni, and Jonathan Oliveira Luiz for their assistance. We express our appreciation to Washburn Shops at WPI for their assistance in machining parts, particularly to Kelli Huang, Jacob Palosky, and Thomas Sterrett for their contributions. We would like to thank staff in the Mechanical and Materials Engineering (MME) department at WPI, specifically Peter Hefti and Barbara Furhman for their support.

Finally, our heartfelt appreciation goes to our sponsor, Pratt & Whitney, for their invaluable support and funding, which made our project possible.

Nomenclature

A = Amplitude of motion

E = Interference or elastic modulus

f_n = Natural Frequency

I = Total intensity or moment of inertia

J = Bessel function of the first kind

k = Stiffness

L = Length

m_{eq} = Equivalent mass

M = Mass

M_{ix} = End effector mass

M_2 = Cantilever beam mass

P = Function including x, y, and z directions and time

t = Time

U_o = Complex representation of object beam

U_R = Complex representation of reference beam

$\Delta\Phi_o$ = Phase of the object beam

$\Delta\Phi_R$ = Phase of the reference beam

λ = Wavelength

τ = Duration of camera exposure

ω = Angular velocity

Problem Statement

The goal of this project is to design, realize, and apply a positioner that increases efficiency and reduces the time and cost of holographic testing for aerospace applications. Standard holographic positioning systems used for high resolution optical metrology in aerostructures are located on a fixed coordinate system. These systems meet stability requirements; however, they lack the degrees of freedom necessary to acquire a full scan of large samples. To test the sample holographically, the sample is maneuvered around a stationary positioner. This process requires extensive time and heavy machinery for large samples.

To reduce the cost and time of holographic testing, the positioner must meet four critical objectives. First, it must be able to move a holographic camera around a stationary sample. This will eliminate the need for heavy machinery and reduce the time and of inspection. Second, the positioner must maintain nanometer resolution at critical locations to ensure accuracy and precision of holographic measurements. Third, the positioner must have the degrees of freedom necessary to obtain a full scan of a large stationary sample and inspect the top and underside of the sample. Fourth, the safety of the user and system must be ensured at all critical locations and while the positioner is being moved or adjusted. The positioner must not tip over or pose any safety hazards to its components or the user. By meeting these requirements, the efficiency of holographic testing procedures can be enhanced, ultimately advancing the capabilities of the positioning system and ensuring accurate results for a range of applications.

1.0 Introduction

In the aerospace industry holography is used to test components of engines to ensure that each component is free of defects and flaws before it is used. This is critical to ensure safe operation of aircraft, for example the commercial airplane shown in **Figure 1**, and the safety of passengers, crew, and pilots alike. Rotor blades undergo major stresses throughout their lifetime which can lead to fatigue and eventually failure, so it is critical these components undergo rigorous testing before and during deployment. Different types of fatigue are referenced in **Figure 2**, including cracks, scratches, and overheating (Pons, Aust, 2019). In order to determine if a component is safe, holographic testing is used to find its natural frequencies. If those natural frequencies fall within an allowable range determined by modal analysis, the component is safe for use. If natural frequencies are outside the allowable range, the component is not safe, and the plane to which the component belongs cannot fly.



Figure 1: Pratt & Whitney Boeing 747 SP (Boeing 747SP, 2024)

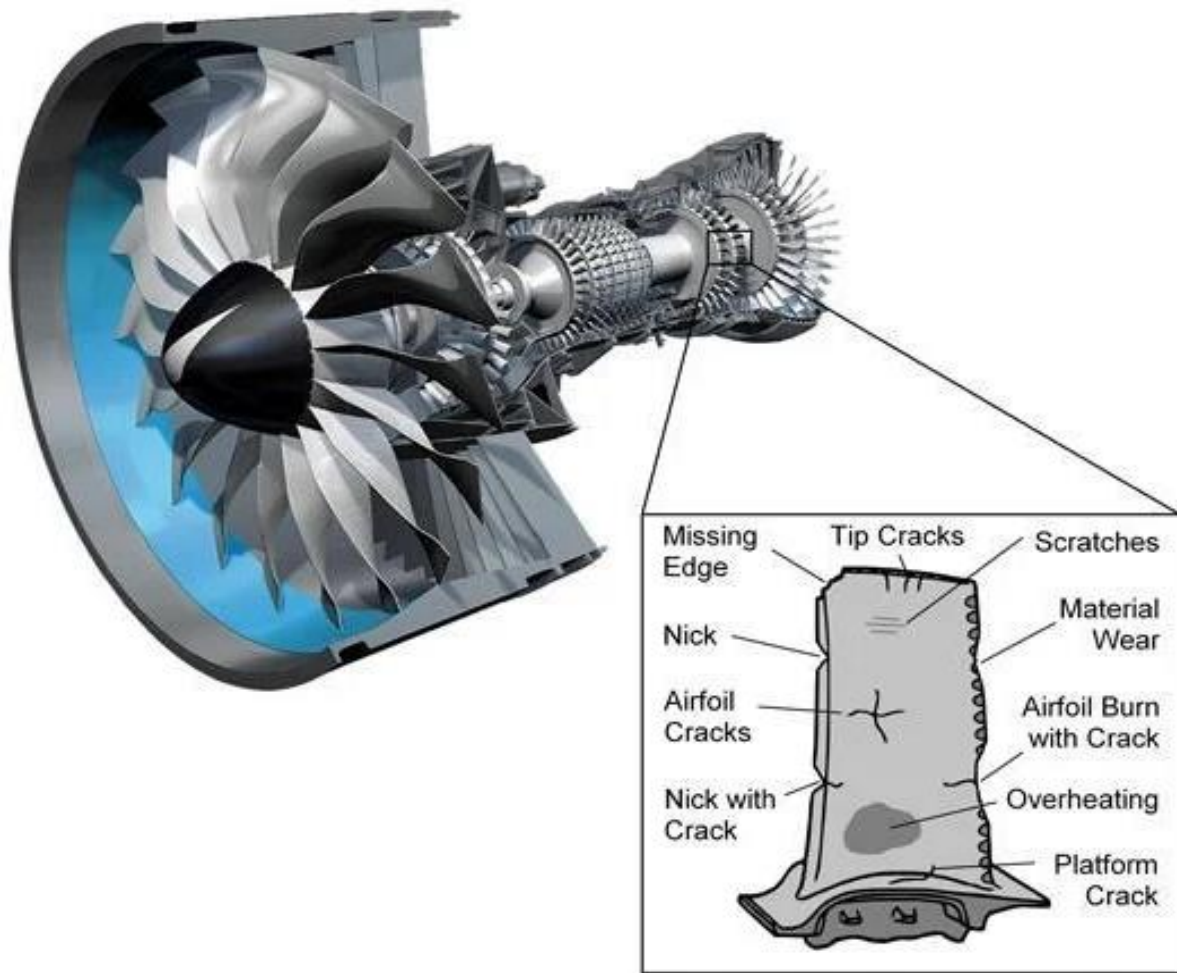


Figure 2: Airplane Engine Fatigue (Pons, Aust, 2019)

In order to perform holographic testing, a positioning system is needed to hold the holographic camera and aim it toward the sample. Current positioning systems for holographic testing rely on a stationary positioning system. This requires the user to move the sample around the positioning system to take holographic measurements at required locations. Many of these samples are large, requiring the use of heavy machinery to move. This increases the time and cost of testing and increases safety risks to technicians who test the sample and the sample itself. To mitigate these risks and reduce the time and cost of holographic testing, this project focused on creating a positioning system that was able to move around a stationary sample while maintaining nanometer resolution for the optical head. This required research on current systems

and the analysis of critical degrees of freedom to determine the proper mechanism for this application. Once a positioner was selected, the system was assembled and tested to determine its natural frequencies and stability. Modifications were then made to the system to shift the natural frequencies of the positioner from the natural frequencies of the sample to ensure the holographic measurements are accurate.

2.0 Background

2.1 Basic Principles of Holography

Holography is a well-known and accepted method of testing in many industries, from medical to aerospace. It allows for the detection of motion in the nanometer range which is not visible through traditional testing methods. A schematic of a typical holographic setup is shown in **Figure 3** below. Holography functions through the use of a single laser that is split into two beams, the object beam and the reference beam. The reference beam is directed to the camera, while the object beam is reflected off the sample and then to the camera. These two beams are compared mathematically for the interference pattern which yields a three-dimensional holographic image showing the deflections in the sample (Pryputniewicz, 1986).

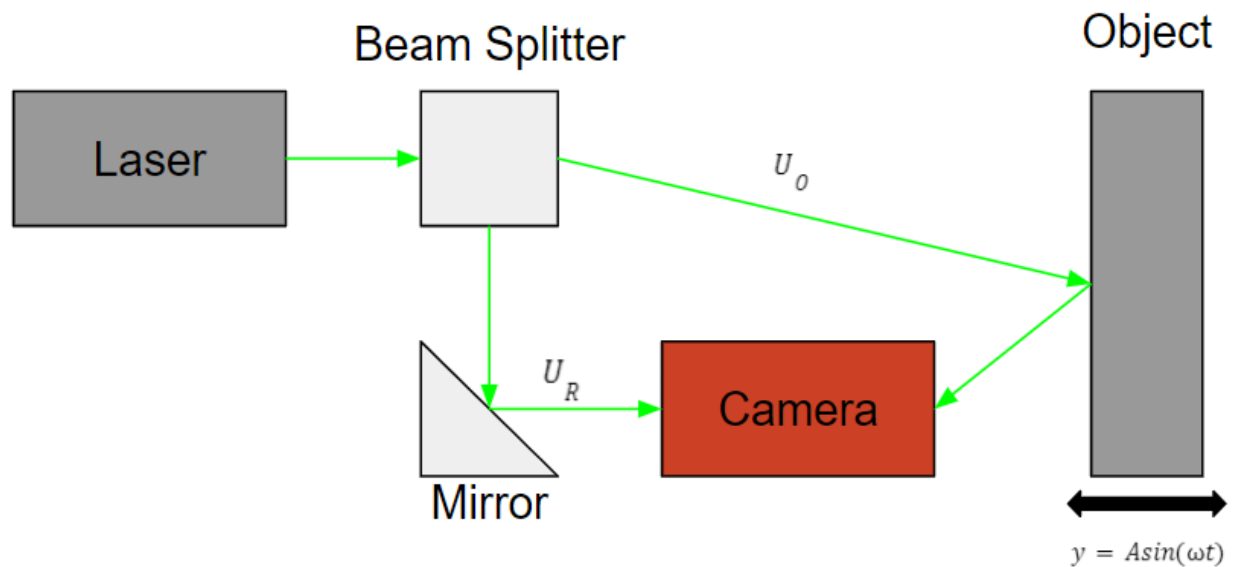


Figure 3: Schematic of Typical Holographic Setup

2.2 Time-Averaged Method for Holographic Vibration Analysis

The intensity of the object beam and reference beam are represented by U_O and U_R . These are complex representations containing both real and imaginary components, shown in **Equation 1** below. The total intensity (I) is the sum of the object beam intensity and reference beam intensity as a function of $P=(x,y,z,t)$, where ϕ =phase, shown in **Equation 2**. The phase of

the object beam (ϕ_o) changes depending on the excitation of the object and is compared to the phase of the reference beam (ϕ_R), which is constant. The resultant phase is extracted from the total intensity equation and used to calculate simple harmonic motion as a function of mass (M), angular frequency (ω ,) and time (t), shown in **Equation 3**. Simple harmonic motion is a sine function showing oscillations in the object during excitation. The sum of the interference and simple harmonic motion equations are integrated by the Zero-Order Bessel Function of the First Kind over the duration of the camera exposure (τ), shown in **Equation 5**. In this function, the frequency is modulated, and the interference (E) and intensity (I) are calculated in **Equations 5-6** and used to produce a three-dimensional holographic image showing deformations of the sample. These equations are integrated into a holographic system that captures images in real time, as follows (Pryputniewicz, 1986),

$$U_O = e^{i\Delta\phi_O(P)} \quad U_R = e^{i\Delta\phi_R(P)}, \quad (1)$$

$$I = |U_O + U_R|, \quad (2)$$

$$y = A\sin(\omega t), \quad (3)$$

$$y = \frac{\lambda}{2\pi} \phi_N = f[M, \omega, t], \quad (4)$$

$$E_{av}(P) = \lim_{T \rightarrow \infty} \frac{E_{01}(P)}{T} \int_0^T e^{i\Delta\phi(P)\sin(\omega t)} dt = E_{01}(P)J_0(\Delta\phi(P)), \quad (5)$$

$$I(P) = I_0(P)J^2(\Delta\phi(P)). \quad (6)$$

2.3 Positioners Used for Holography

An image of the holographic setup used in the CHSLT lab is shown below in **Figure 4**. This setup contains a positioner that holds a holographic camera and green laser that illuminates a rotor. The rotor is attached to a piezoelectric shaker that excites the rotor by producing specific programmed frequencies. This positioner meets stability requirements to maintain nanometer resolution for the optical head; however, it lacks the degrees of freedom necessary to acquire a

full scan of stationary rotor samples. To capture holographic images at different locations, the rotor sample needed to be rotated and moved around the positioning system. This posed a need for a new positioner able to meet all stability and maneuverability requirements.

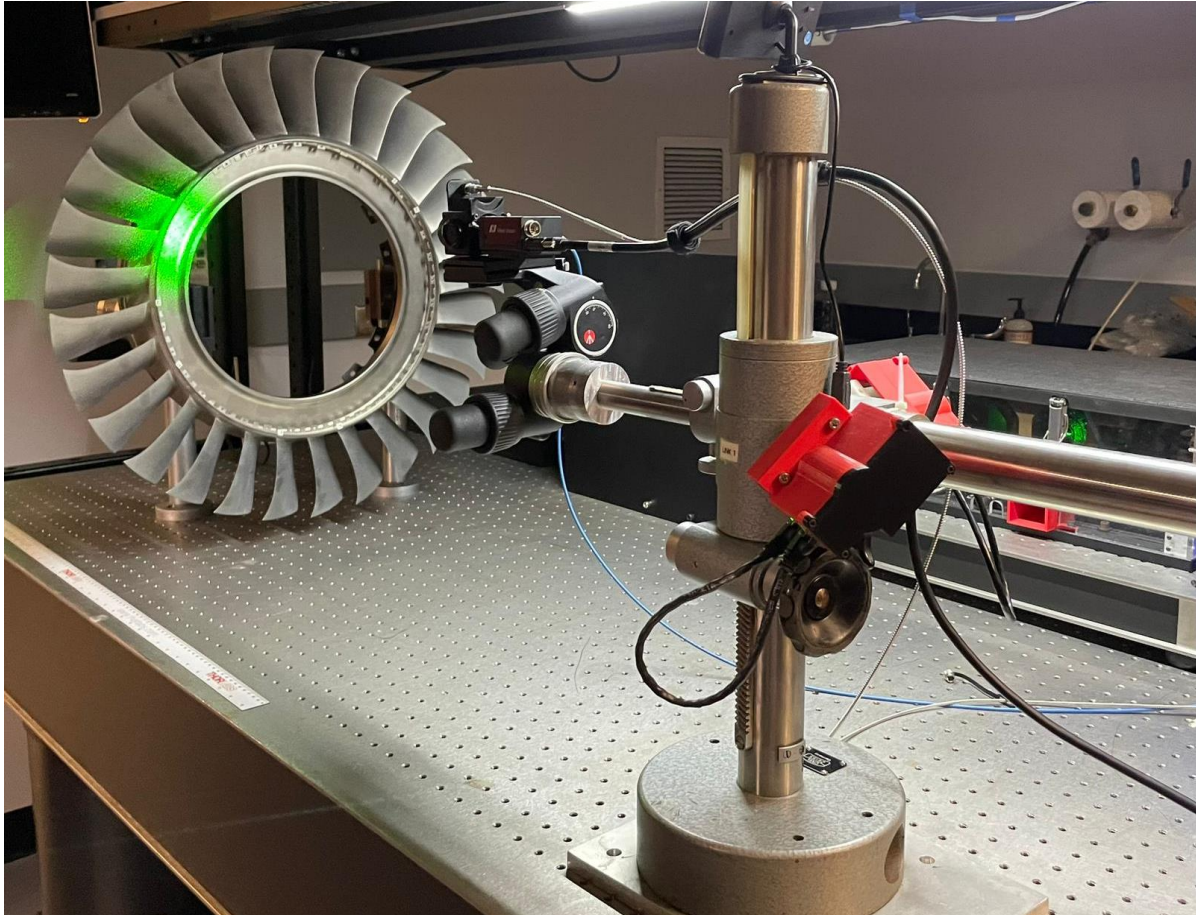


Figure 4: Holography Setup Used in CHSLT Lab at WPI. Positioner is Constrained Requiring the Movement of Sample Around Positioner. For Larger Components, it is Desirable to Keep Object Fixed and Move Holographic Camera Around Object for Inspection to Minimize Inspection Time and Cost.

3.0 Methodology

3.1 Methodology

The basic layout of the methodology is shown in a flowchart in **Figure 5** below. This project began with research on positioners used for holographic testing and similar applications, including surgery and photography. Then the objectives, constraints, and functional specifications of the desired positioning system were determined. This information was used to determine degrees of freedom necessary for the positioning system. Once these degrees of freedom were identified, analysis could begin. This started with analytical modeling of an idealized positioner to determine the natural frequencies of potential positioning systems. This narrowed down selection of a system by ruling out systems that did not fit stability requirements. Computational modeling was performed on potential components to gather further data on whether the potential components would fit the criteria. Components were determined from the list of components and purchased. One of these components allowed for vertical translation, and the other allowed for horizontal and vertical translation.

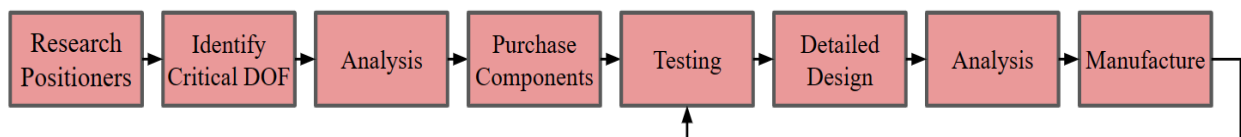


Figure 5: Flowchart of the Methodology Used in this Project

Through testing it was determined that the vertical stand was acceptable; however, modifications were necessary to combine the two components successfully. This began the iterative process that guided the remainder of the project. Following the testing, detailed design was performed in SolidWorks. This included modeling both the vertical and horizontal stands in detail, which required the disassembly and measuring of every component of the stands. Once this was complete, a plate could be designed to combine the two. This plate was analyzed using simulations in SolidWorks to determine if it would meet the necessary requirements. Once designed and analyzed, this component was manufactured at Washburn Shops.

Once all components were obtained and assembled, the process iterated again beginning with testing, moving through a modified detailed design, analytical and computational simulations, and manufacturing. A testing setup was developed to determine the natural frequencies of the positioning system to ensure the accuracy of the simulated results and the stability of the system. It was determined that further modifications were needed to ensure stability of the system. These were then detailed, simulated, and compared to the original results. Once the parts were deemed acceptable, they were then manufactured again at Washburn Shops and implemented into the system. From there the system looped again back to testing to ensure the parts accomplished the objectives that they were designed for.

A Gantt chart was made to ensure the project stayed on schedule for the duration. This was done through determining milestones and their corresponding activities for each term, shown in **Appendix 1**. In the first term, efforts were concentrated on problem definition and extensive research. Moving into the second term, focus was shifted towards conceptualization and idealization. In the third term, there was a transition to prototyping and the development of the positioning system. Finally, in the fourth term, attention was dedicated to rigorous testing and evaluation of the system's performance.

3.2 Constraints and Functional Specifications

Constraints are limitations that need to be adhered to, whereas functional specifications are capabilities that the final system must have. **Appendix 2** provides two tables delineating the project's constraints and functional specifications. Below, **Table 1** exemplifies a constraint from **Appendix 2**. In the first (leftmost) column, constraints were split into four categories: operation, safety, cost, and structure. In the five remaining columns, the part, description of the part, constraint, level of importance of the constraint, and reasoning for level of importance were identified. The bottom row shows an example of a structural constraint, the ten-kilogram weight limit of the cantilever positioner (Polytec stand). This constraint was ranked as most important because it is a property of the Polytec stand that put limitations on the weight of the positioning mechanism on top of it. Other important constraints included budget, safety requirements for the system components and operator, as well as the stability requirements of the system. The most

important functional specifications included the cost of components and the positioner’s ability to move without risking safety.

Table 1: Example of a Constraint Taken from Appendix 2

Constraints					
Category	Part	Description	Constraint	Level of Importance (1=most important, 5=least important)	Reasoning
Structure	Cantilever Positioner	Weight Limit	-10kg (22lbs)	1	Property of the Polytec Stand

3.3 Positioner Selection

A kinematic model, shown in **Figure 6**, was created to visualize parameters, allowing for the determination of the requirements for implementing each potential degree of freedom. The kinematic model facilitated the visualization of how the positioner would move around the stationary sample to inspect it at different positions. Research was conducted on potential systems that would satisfy maneuverability and stability requirements. These mechanisms included a single arm boom stand, a balanced four bar mechanism, and an articulating arm, shown in **Figure 7**. The single arm boom stand satisfied stability requirements but did not satisfy maneuverability requirements. The articulating arm satisfied maneuverability requirements but did not satisfy stability requirements. Lastly, the balanced four bar mechanism satisfied both requirements.

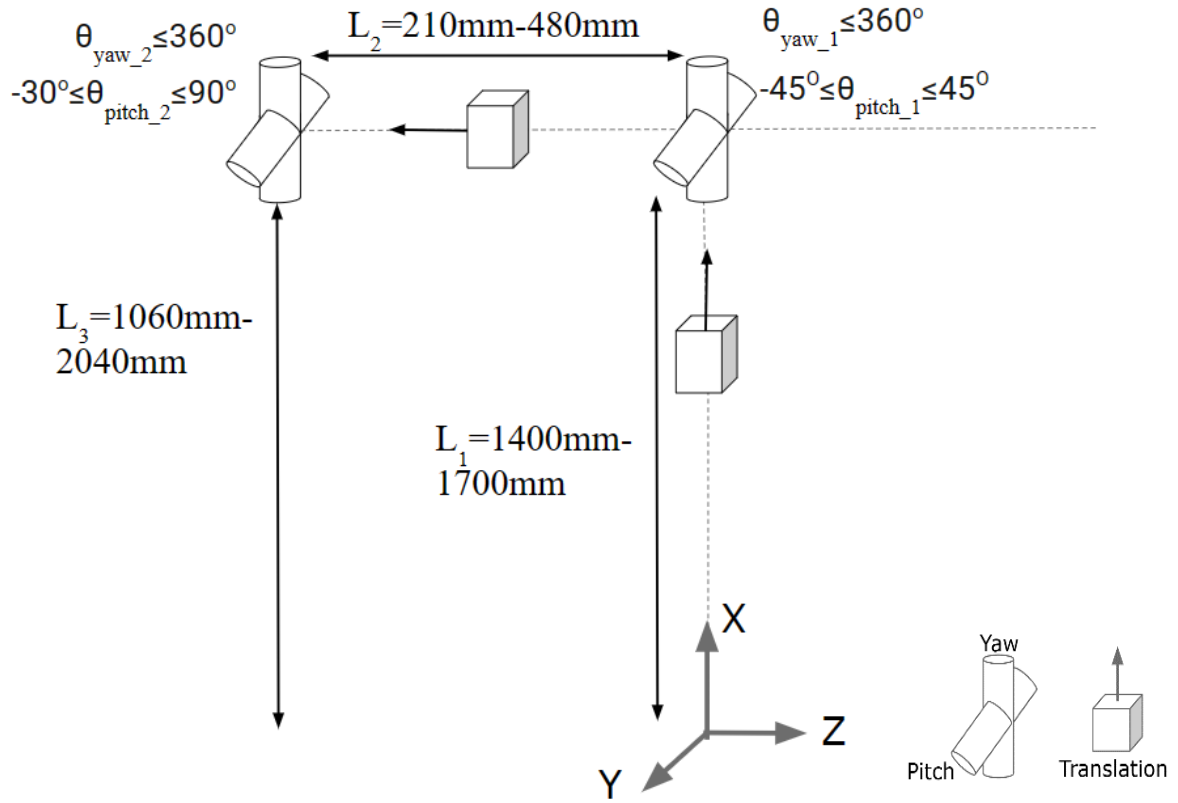


Figure 6: Kinematic Model of Mechanism with Required DOFs



Figure 7: Considered Mechanisms to Satisfy Necessary DOFs, Boom Stand (Scienscope, 2024), Balanced Four Bar (Edelkrone, 2024), and Articulating Arm (FX Articulating Arm, 2024)

The advantages and disadvantages of each positioning mechanism were compared to determine which mechanism to purchase. The requirements satisfied by the three mechanisms were compared in **Table 2** and ranked by level of importance with one being least important and five being most important. The single arm boom stand met four of the six specified requirements. The balanced four bar mechanism met all six requirements. The articulating arm met five requirements. The balanced four bar mechanism was the only mechanism to meet all requirements, so it was selected over the other two mechanisms.

Table 2: Requirements Satisfied by Boom Stand, Balanced Four Bar, and Articulating Arm

Requirements for Mechanism	Level of Importance (1=most, 3=least)	Requirements Met by Single Arm Boom Stand (Y/N)	Requirements Met by Balanced Four Bar (Y/N)	Requirements Met by Articulating Arm (Y/N)
When the mechanism is moved, it must be safe for technician and its system components	1	Y	Y	Y
Mechanism must fit within the budget of entire Pratt & Whitney order	1	Y	Y	Y
Mechanism must hold the optical head while maintaining nanometer resolution	1	Y	Y	N
Mechanism must be able to maneuver optical head around a stationary sample	1	N	Y	Y
Mechanism must be able to pitch and yaw at the base	2	N	Y	Y
Mechanism must be able to move in the Z-direction	3	Y	Y	Y

Three components were selected to create the positioning system. The first component was the Polytec stand, specifically designed for optical metrology. This component added a

course degree of freedom, motion in the vertical direction designated by X in the chosen frame of reference. The second component was the Edelkrone JibONE, a balanced four bar mechanism. This component was designed for photography and added the course degrees of freedom of horizontal extension, the designated Z direction, as well as pitch and yaw. Since this component was designed for applications that did not require the same stability as holography, structural modifications were made to its base and end effector. The third component was a Monfrotto camera mount. This component added two fine degrees of freedom, pitch and yaw.

The balanced four bar mechanism was integrated into the holographic inspection system, shown below in **Figure 8**. A damped optical table supports a piezoelectric shaker and the positioner. A representative commercial rotor sample from Pratt & Whitney is horizontally on top of the piezoelectric shaker. The positioner is composed of the Polytec stand, JibOne, counterbalance, camera mount, holographic camera, and a modified base and end effector. The holographic camera points toward the rotor in the Y-direction.

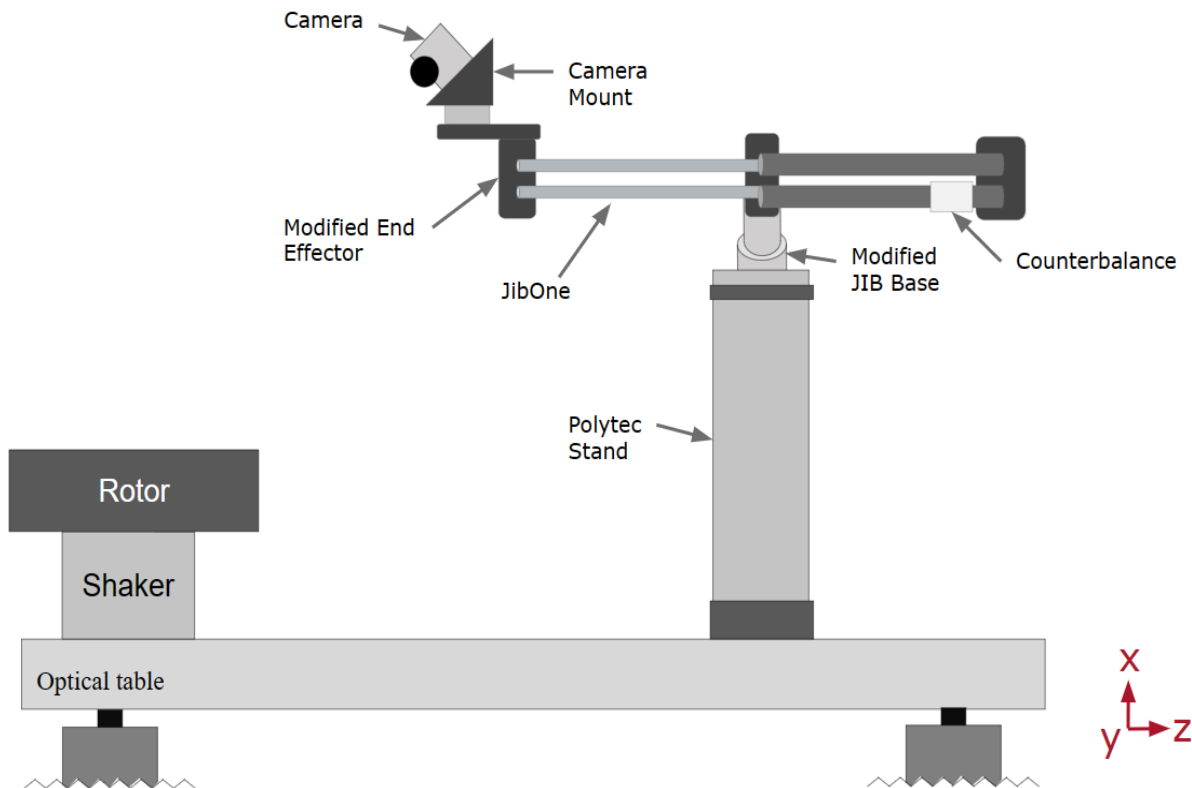


Figure 8: Mechanism Integrated into Holographic Inspection System

An idealized model of the balanced four bar mechanism is shown below in **Figure 9**. The natural frequency (f_n) of the cantilever arms with end masses was calculated in **Equation 7** from the stiffness (k) calculated in **Equation 8** and equivalent mass (m_{eq}) calculated in **Equation 9**,

$$f_n = \frac{1}{2\pi} \sqrt{\frac{k}{m_{eq}}}, \quad (7)$$

$$k = \frac{3EI}{L^2}, \quad (8)$$

$$m_{eq} = M1 + (33/140)M2. \quad (9)$$

Uncertainty analysis was used to rank the effect that each parameter had on the natural frequency. The length (L) had the greatest effect, cross sectional dimensions (m_{eq} , I) had medium effect, and the elastic modulus (E) had the smallest effect. The mass and position of the counterbalance also impacted the natural frequency. All factors had to be considered to tune the positioner so that its natural frequencies had minimal effect on stability.

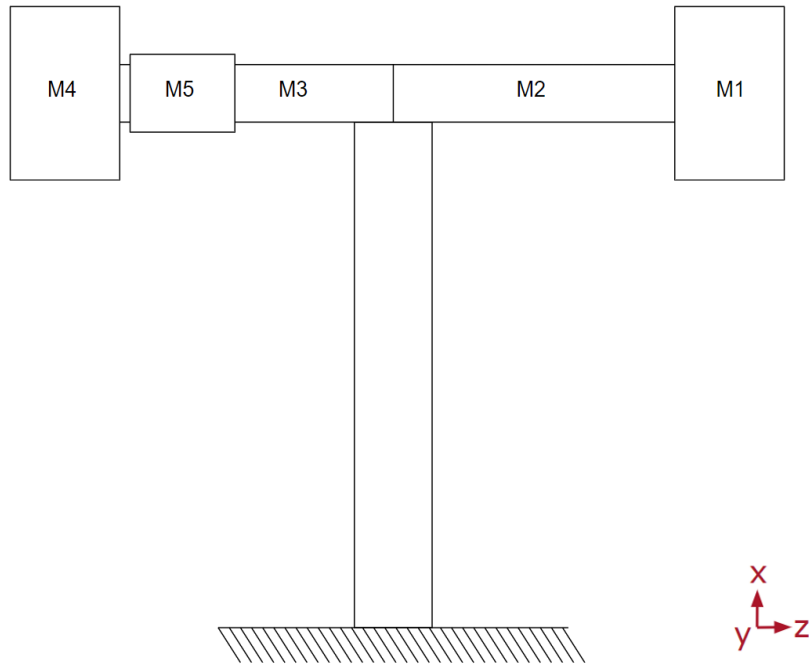


Figure 9: Idealized Model of Selected Mechanism Including Mass Representing End Effector and Mass Representing Counterbalance Weights

3.4 Computational Modeling

3.4.1 Detailed Design

Detailed models of the positioning system before and after modifications are shown in **Figures 10-11** below. Each model contains the Polytec stand, balanced four bar mechanism, camera mount, and optical head. The Polytec stand, balanced four bar mechanism, and camera mount were modeled with the same materials, dimensions, and degrees of freedom as the real positioning system with millimeter resolution. The optical head was modeled with the same center of gravity and weight as the real optical head. These models allowed for the determination of highly accurate and precise simulations.

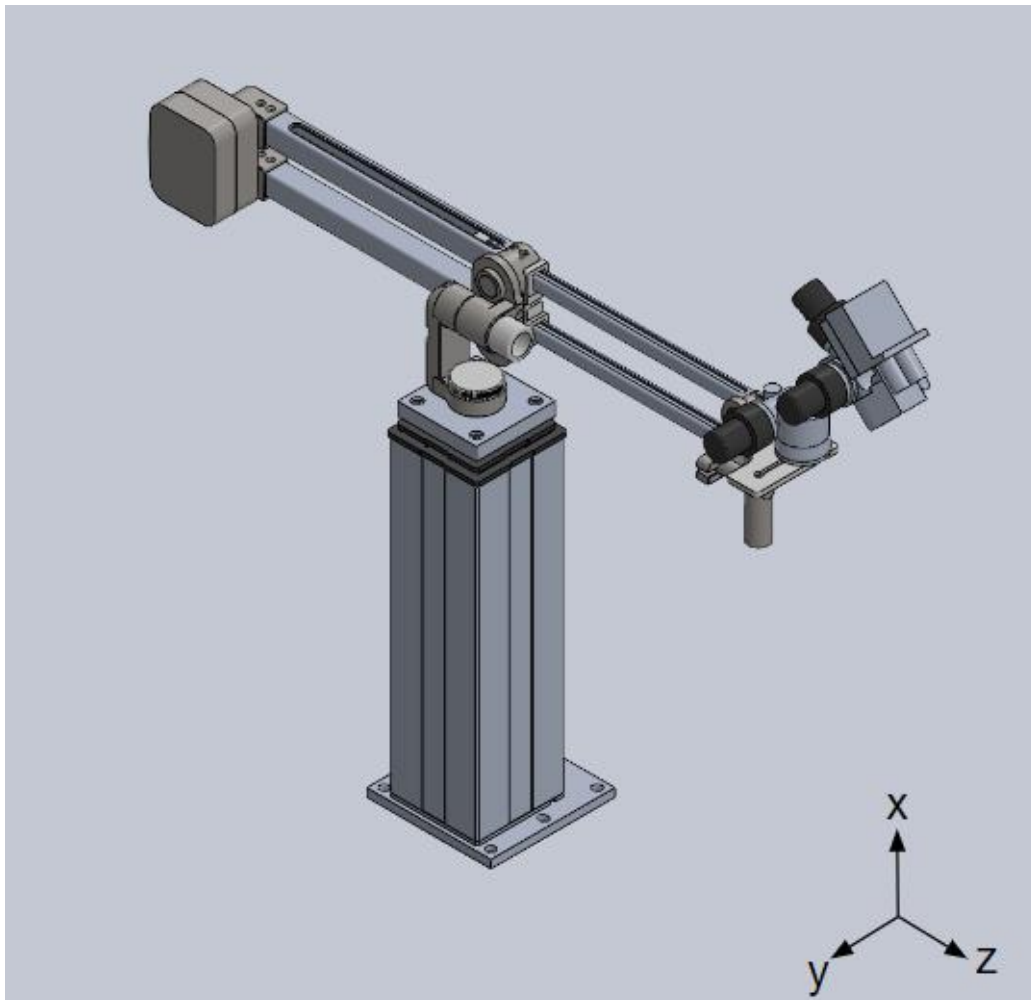


Figure 10: Detailed SolidWorks Model of Unmodified Positioning System

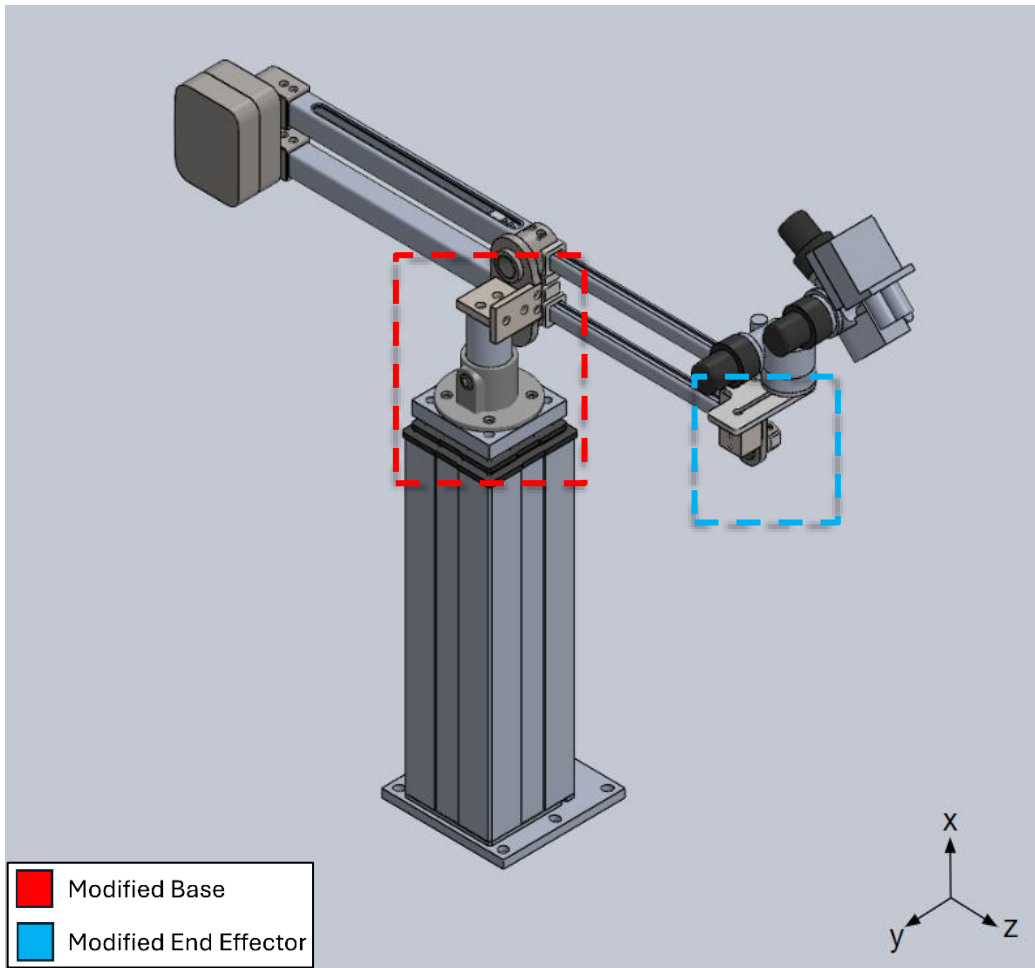


Figure 11: Detailed SolidWorks Model of Modified Positioning System. Modifications Include a New Base of the Four Bar Mechanism (Highlighted in Red) and a New End Effector Connection (Highlighted in Blue) Obtained Through Analysis While Accounting for the Structural and Dynamic Characteristics of the Positioner to Minimize Structural Effects on the Holographic Measurements.

3.4.2 Parametric Analyses

To determine the modifications needed, a simplified balanced four bar mechanism was modeled in SolidWorks and a variety of Finite Element Analysis simulations were conducted. Simulations determined the factors of safety, stress, strain, resultant displacement, displacement in the X-, Y-, and Z- directions, and the first twelve natural frequencies of the unmodified positioning mechanism. Next, SolidWorks models were created of the mechanism with a modified base only, a modified end effector only, and a modified base and end effector. The same simulations were performed for these three models. The scales for each type of simulation

were adjusted to have the same colors and range. The simulations performed on the unmodified mechanisms were compared to those performed on the modified mechanism to determine the effect that each modification had on stability, shown in **Appendix 3**. The factor of safety of the unmodified mechanism is shown in **Figure 12** and that of the modified mechanism is shown in **Figure 13**. These simulations showed the stability of the system increased with the modifications.

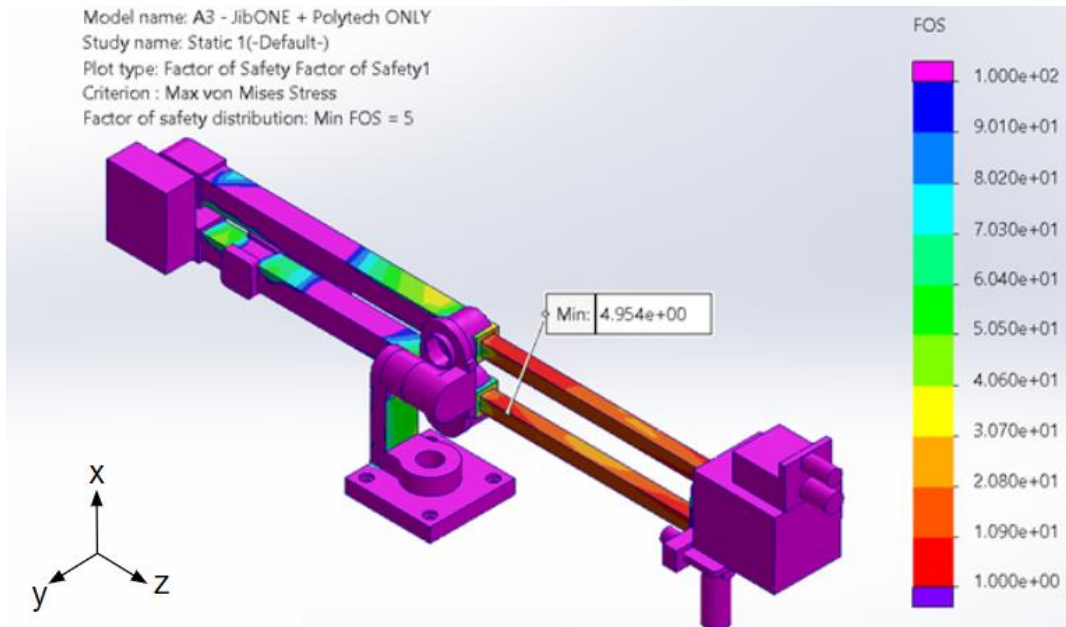


Figure 12: Safety Factor of the Unmodified Mechanism From 4.954 to over 100.

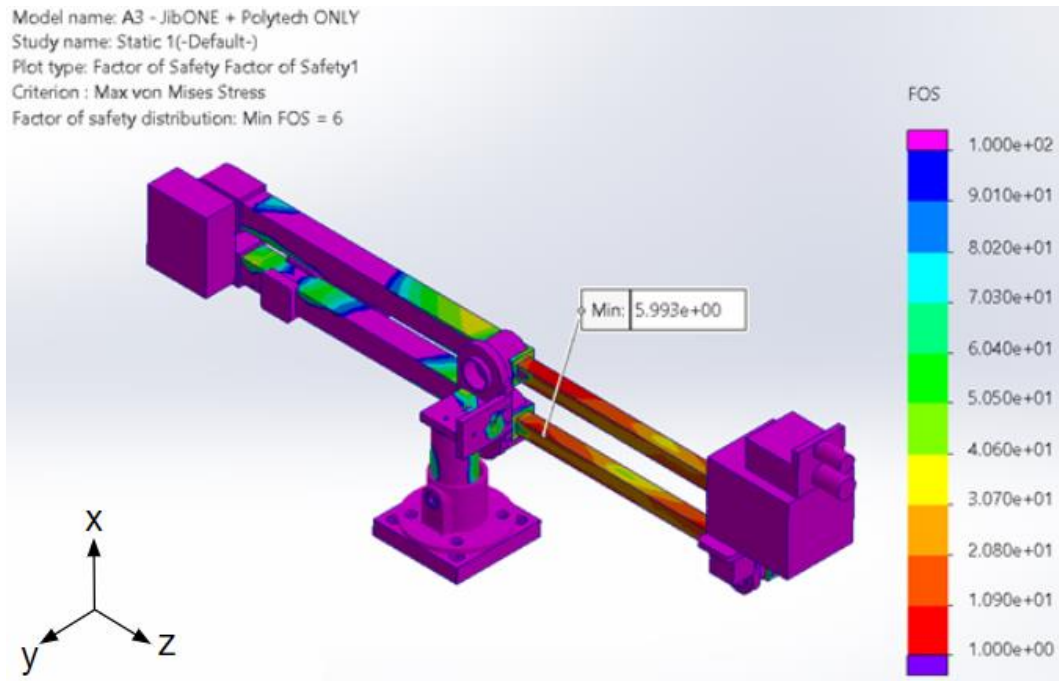


Figure 13: Safety Factor of the Modified Mechanism From 5.993 to over 100. This Shows an Increase in the Safety Factor Along the Extended Bars Holding the End Effector.

Modal analysis simulations were performed for the first twelve mode shapes on the balanced four bar mechanism before and after modifications, shown in **Appendix 4**. The X-, Y-, Z-, and resultant components were captured for each mode. Below, **Table 3** shows the X-, Y-, Z-, and resultant components for the first mode shape of the unmodified four bar mechanism and **Table 4** shows those of the four bar mechanism with a modified base and end effector. The natural frequencies of the system were plotted in **Figure 14**. This graph shows that the natural frequencies increased with a modified base and end effector. Overall, however, the natural frequencies were in the lower range; therefore being removed from typical natural frequencies of rotor blades. Based on these findings, a new base and end effector were manufactured and assembled into the positioning system.

Table 3: X-, Y-, Z-, and Resultant Component for Mode 1 of the Balanced Four bar Mechanism Before Modifications

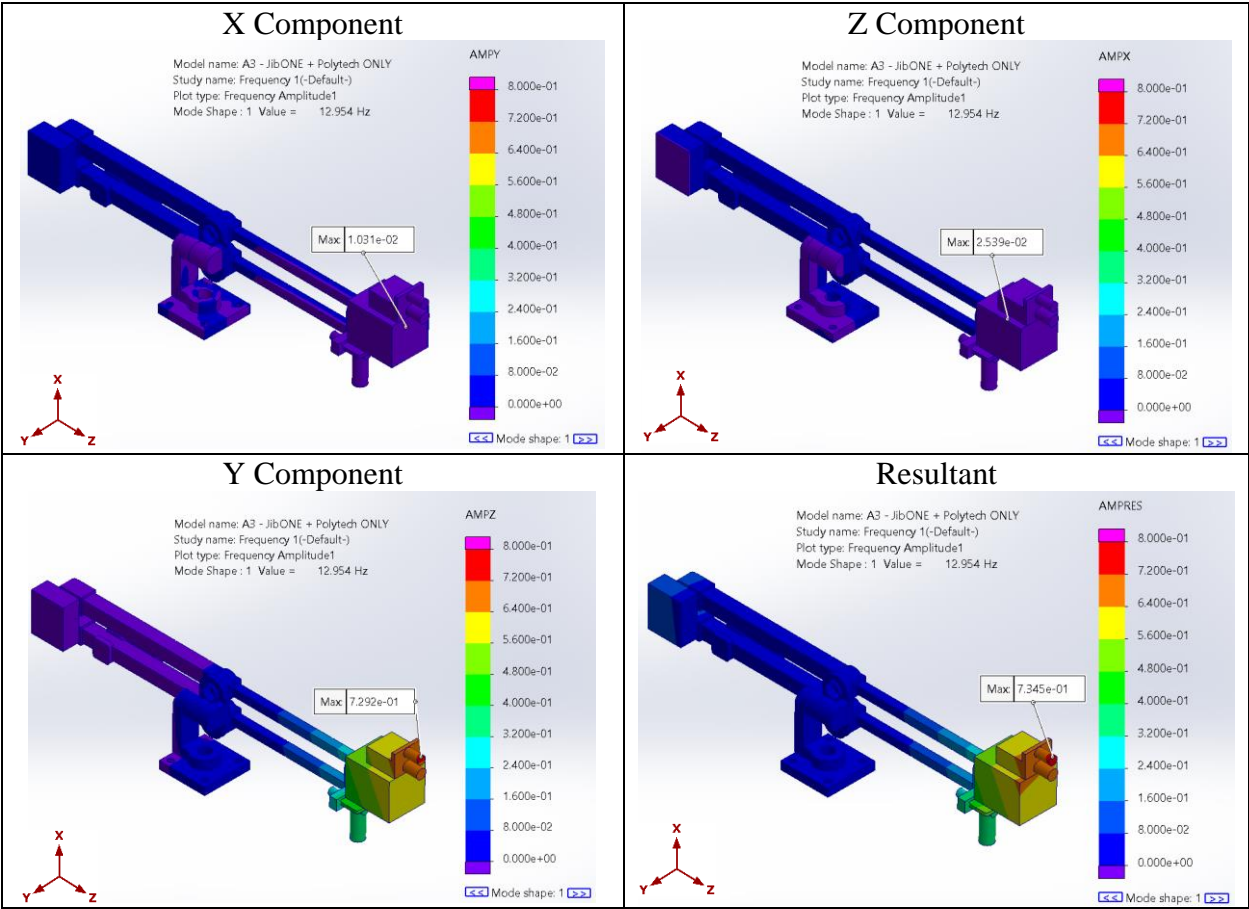


Table 4: X-, Y-, Z-, and Resultant Component for Mode 1 of the Balanced Four bar Mechanism with a Modified Base and End Effector. The Mode Shapes are Consistent Before and After Modification, With a Frequency Shift.

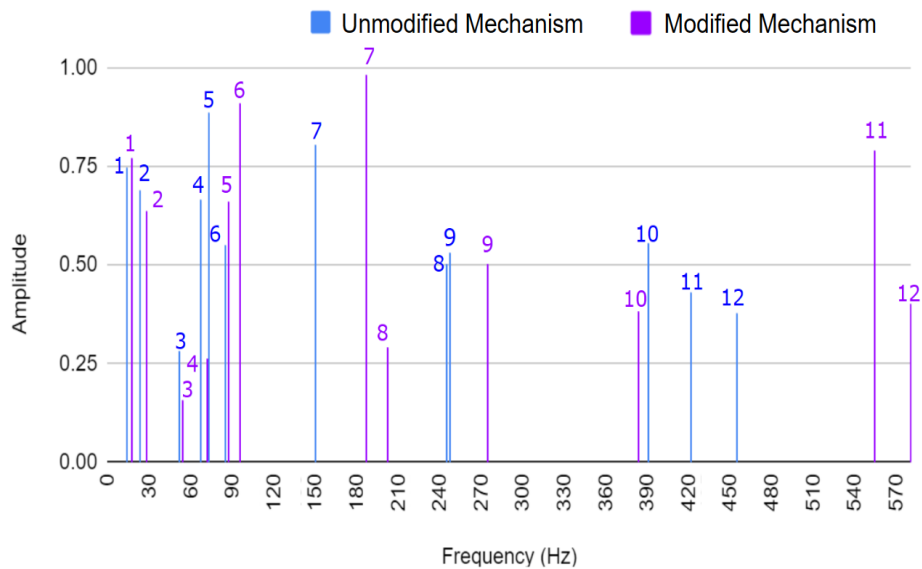
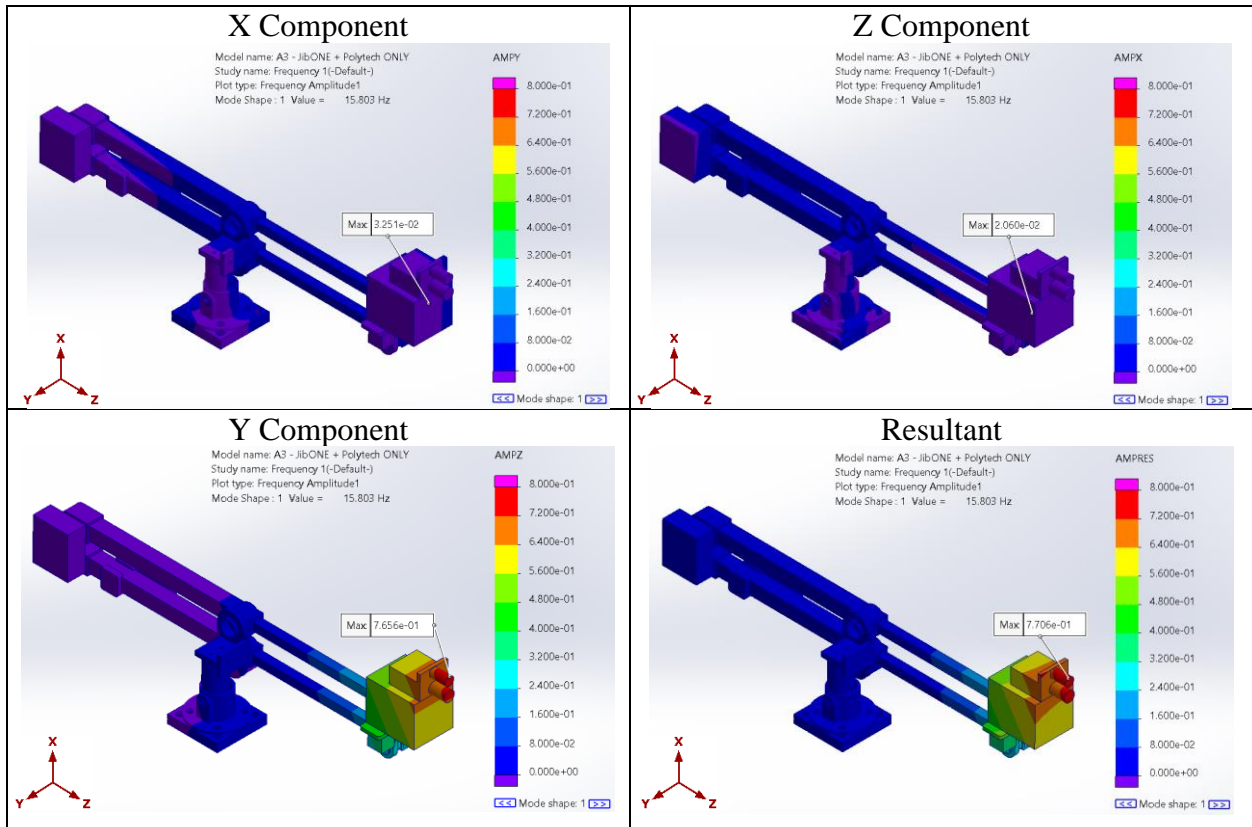


Figure 14: Predicted the Shift of the Natural Frequencies After Structural Modifications. This Shows an Overall and Complex Increase in Natural Frequencies Post Modification While Maintaining Low Natural Frequencies When Compared to Sample.

3.5 Experimental Validation and Testing

3.5.1 Impact Testing with Three Laser Doppler Vibrometers

A testing method was developed to determine the resonant frequencies of the positioner before and after modifications using an impact hammer and three Laser Doppler Vibrometers (LDVs). LDVs are devices that use the Doppler effect to measure the velocity of vibrating surfaces in order to characterize their vibration behavior. The test setup, shown in **Figure 15**, shows three LDVs aimed along each axis to evaluate motion of the optical head in the X-, Y-, and Z-direction. Each LDV was directed to a piece of reflective tape on the camera head, shown in **Figure 16**.

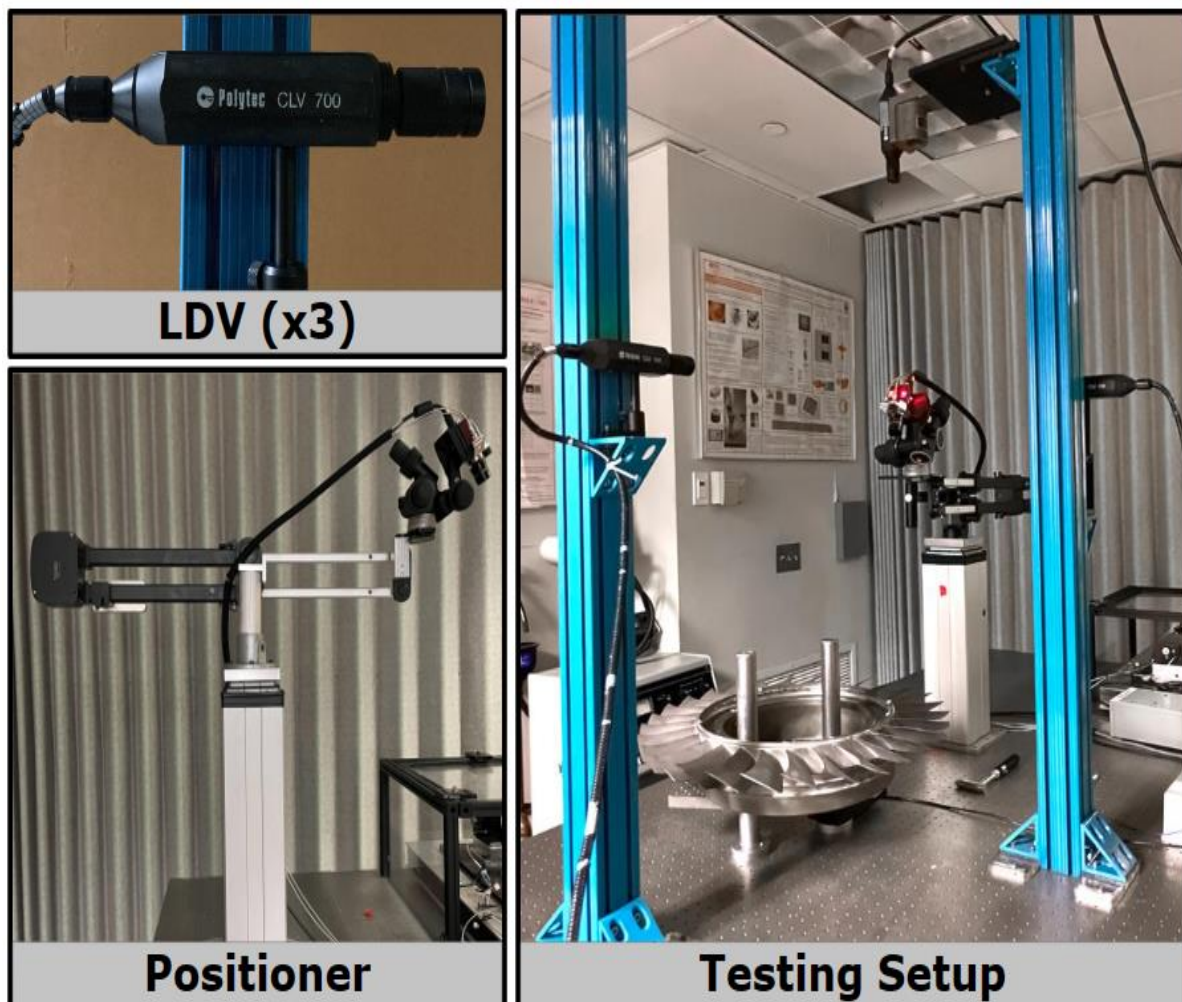


Figure 15: Testing Setup with LDVs and Positioner.

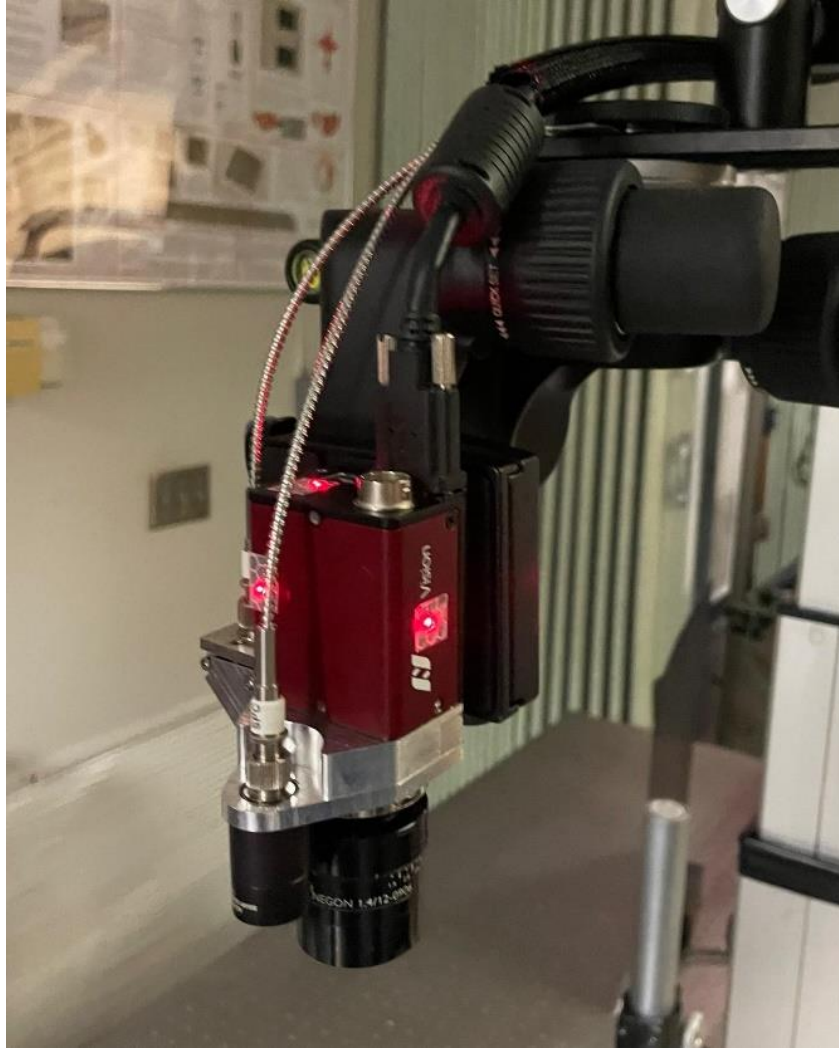


Figure 16: Three LDV Lasers Aimed at the Optical Head in the X-, Y-, and Z- Directions.

In order to gather the data, LabVIEW software was used, as shown in **Appendix 5**. This required the use of a National Instruments data acquisition module (DAQ), the NI USB-6229-BNC. This device was connected to the rest of the system six ways. The first was to a computer using a USB A to USB B cable. It was also connected to each LDV, the LDV X direction being connected to port AI3, the LDV in the Y direction was connected to the AI1, and the Z-directional LDV was connected to the AI2 port. The AI3 port was connected to a Dyrion Current Source which acquired signals from the impact hammer. The entire system was plugged into a 120V outlet, referred to here as a power source. Along with being connected to the DAQ, the LDVs, current source, and computer were also connected to a power source. Lastly, the impact hammer was

connected to the current source. All of this is shown through a diagram in **Figure 17** and visually in **Figure 18**. Below, **Table 5** shows the components used for this testing.

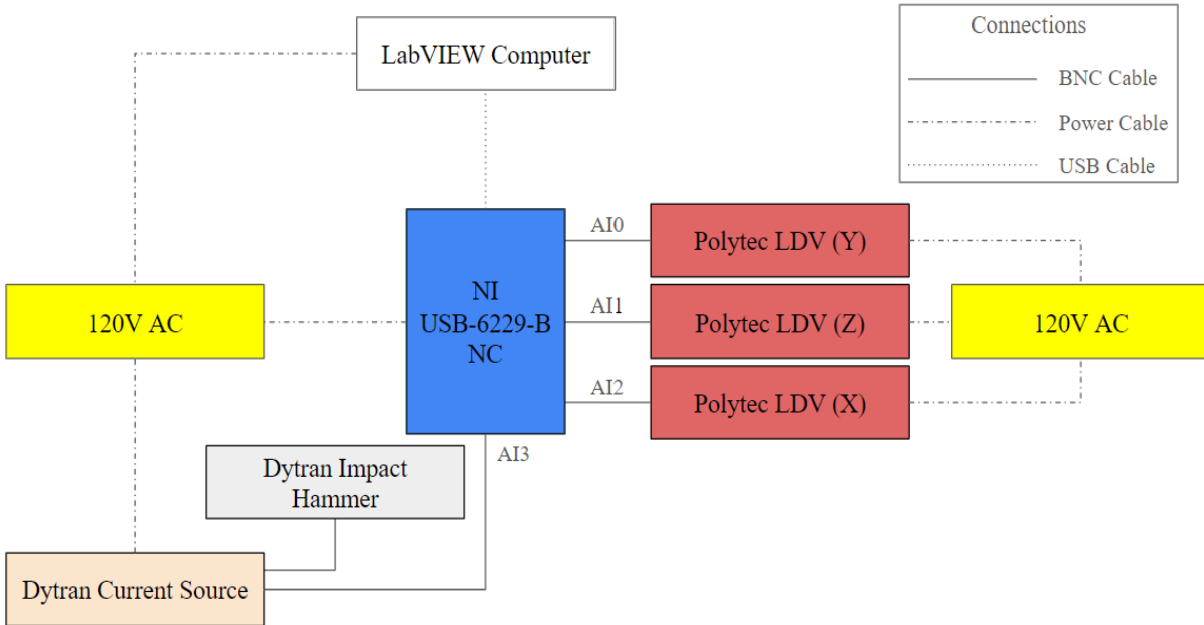


Figure 17: Wiring Diagram of LDV Setup.

Table 5: List of Devices Used for Impact Hammer Testing

Device	Manufacturer, Model Number
DAQ National Instruments	NI, USB-6229-B NC
DAQ Moku:Lab device	Liquid Instruments, WL18MODGI
Vertical Test Stand PSV (110V)	Polytec, PSV-A-T18
Laser Doppler Vibrometer Controller 1	Polytec, CLV 1000
Laser Doppler Vibrometer Controller 2	Polytec, CLV 1000
Laser Doppler Vibrometer Controller 3	Polytec, CLV 1000
Laser Doppler Vibrometer Laser Head 1	Polytec, CLV 700
Laser Doppler Vibrometer Laser Head 2	Polytec, CLV 700
Laser Doppler Vibrometer Laser Head 3	Polytec, CLV 700
Dytran Current Source Power Unit	Dytran, 4112B
Impulse Hammer	Dytran, 5850B
Dual mode Amplifier	QSC, CX302
3-axis accelerometer w/ analog volt outputs	Analog Devices, ADXL326

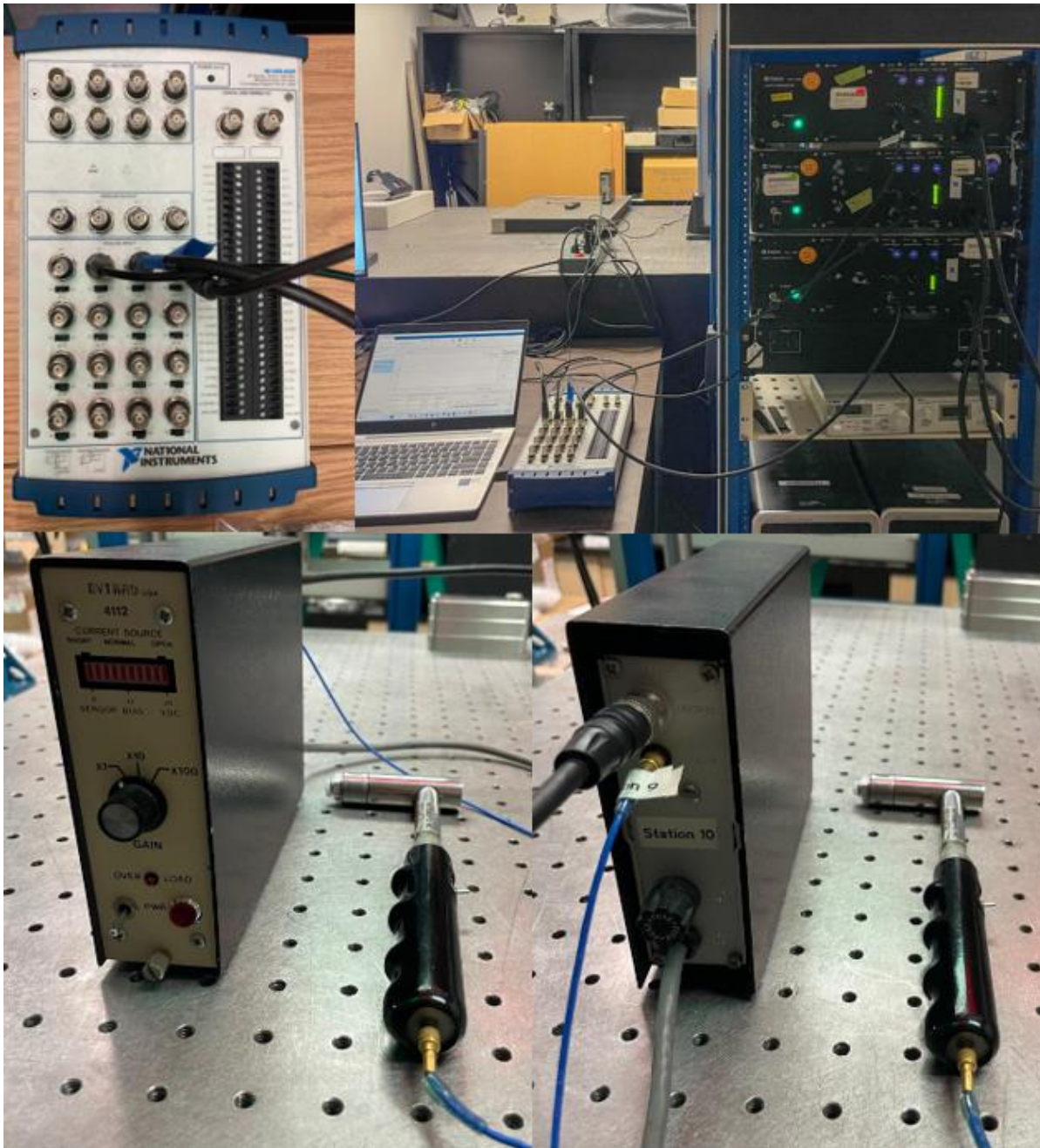


Figure 18: Visual Wiring Connections. NI Shown Top Left, LDVs Shown Top Right, Current Source Bottom Left and Impact Hammer Bottom Right.

Another transducer explored was the accelerometer, shown in **Figures 19 and 20**. An accelerometer was glued to the side of the Polytec stand, parallel to the XZ plane. It was used to measure the acceleration in the X-, Y-, and Z-direction when the positioner system was excited. The velocity of the vibrating camera head was determined from the acceleration. The accelerometer was connected to four wires to transmit power and data. Vibrations in the Polytec

stand caused movement in these wires, leading to inaccurate measurements. The Laser Doppler Vibrometers did not need to touch the positioning system to record its vibrations. They were used instead of accelerometers because they had greater accuracy in their measurements.

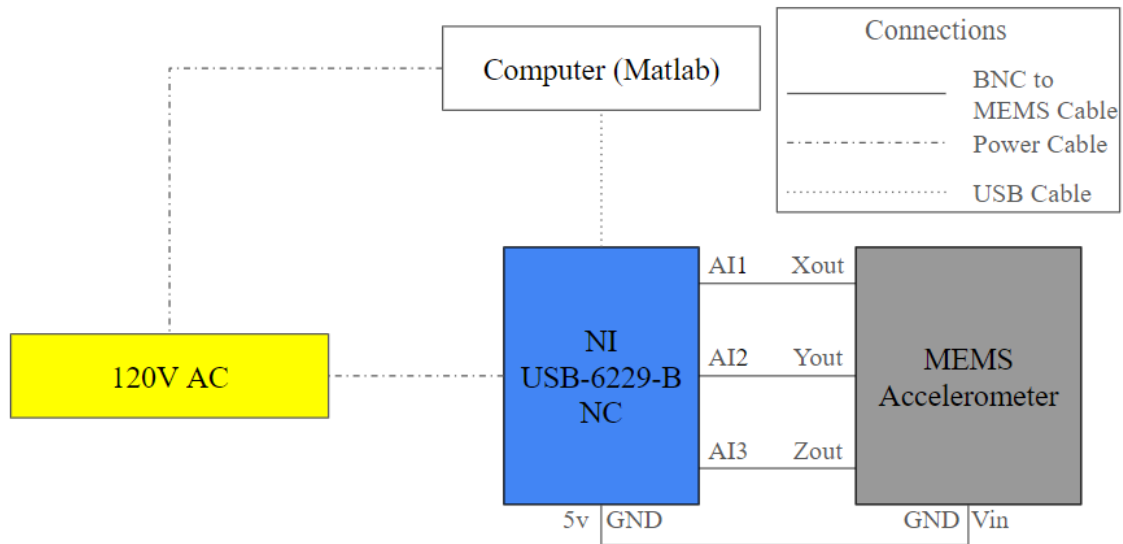


Figure 19: MEMS Accelerometer (ADXL 326) Wiring Diagram.

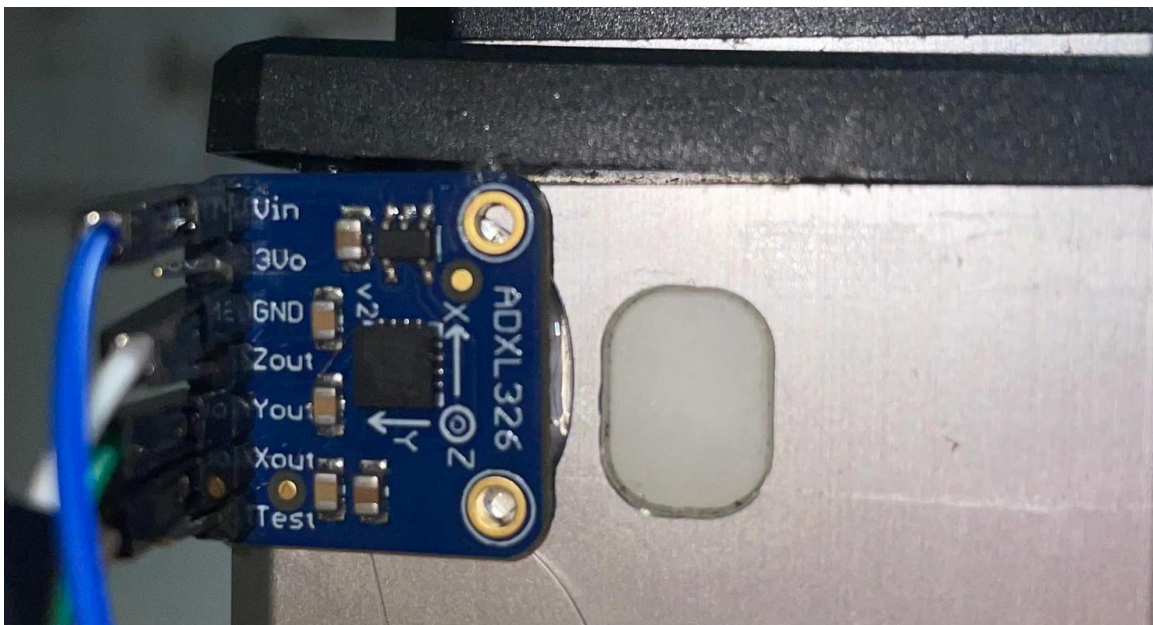


Figure 20: MEMS Accelerometer (ADXL 326) Attached to the Polytec Stand.

This required the excitation of the sample in all three directions, which was accomplished using an impact hammer. The impact zones were marked with red tape on the positioner in the Y- and Z- directions and on the table in the X-direction. The impact hammer and the impact zone in the X-direction is shown in **Figure 21**. These three zones were then each struck to excite the optical head, once by the hammer with a thirty second delay between impacts. Simultaneously, a live LabVIEW program was averaging the FFTs of the impacts to gather information about the natural frequencies in each direction. This was done before and after modification to ensure the modifications corroborated the theoretical analysis.

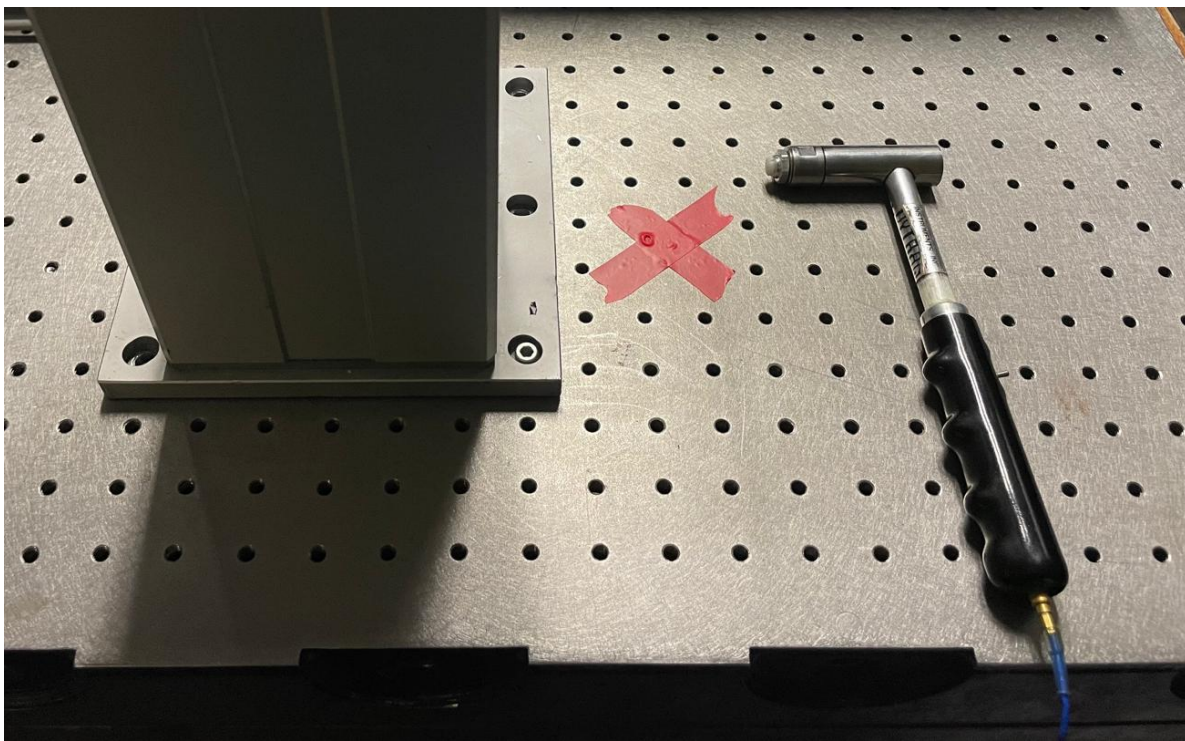


Figure 21: Impact Hammer Next and Impact Zone in the X-Direction Marked in Red Tape.

In LabView, Fast Fourier Transformers (FFT) were applied to the data collected by the three LDVs, which allowed the determination of the natural frequencies of the positioner. This information was used to ensure the modified base and end effector shifted the frequencies of the positioner away from the frequencies of the sample being tested. The results are shown in **Figures 22-24**. These figures support the computational models by showing an increase in the frequencies overall, as well as most of the frequencies being represented in the lower range. **Figure 22** shows the responses in the x-direction, with the first three pre modification natural

frequencies being 4Hz, 13Hz, and 24Hz. Post modification, these were 6Hz, 9Hz, and 36Hz. This shows an overall increase in the frequencies post modification.

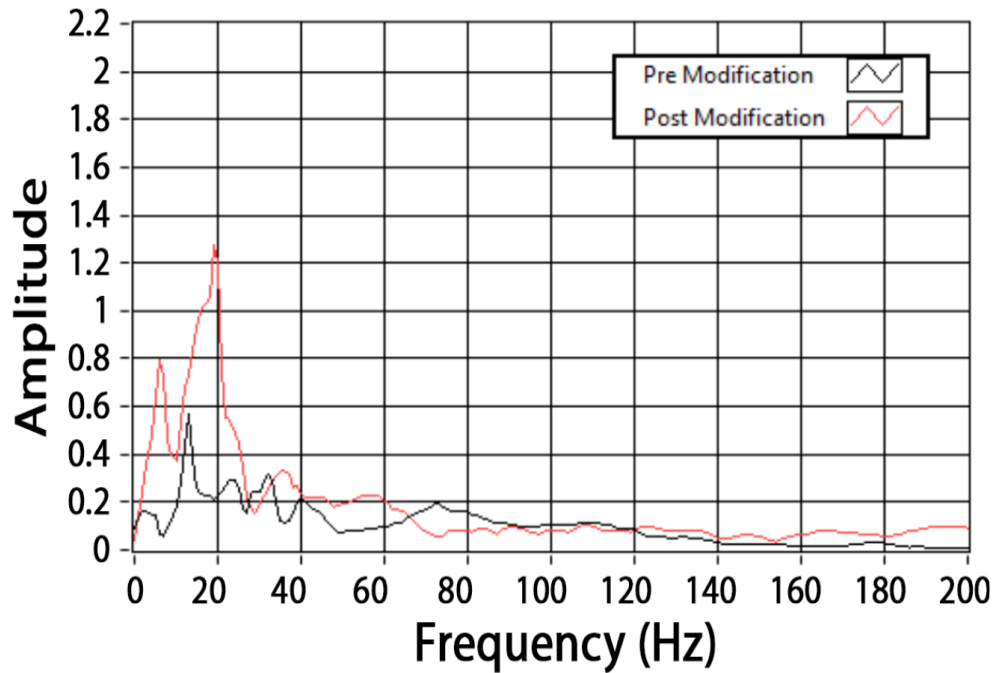


Figure 22: Frequency Responses in the X-Direction.

The y-directional frequency responses represented in **Figure 23** show a slightly different trend, in which the frequencies represented stay relatively similar, with pre modification frequencies being 5Hz, 13Hz and 29Hz. The post modification values were 5Hz, 12Hz, and 25Hz. This shows a slight decrease in frequencies in the y-direction.

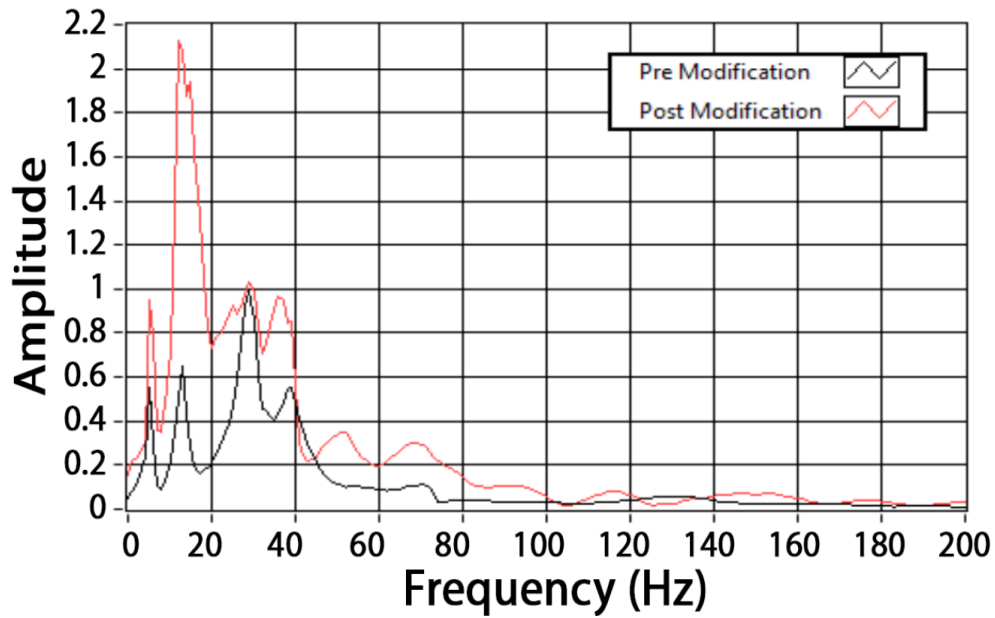


Figure 23: Frequency Responses in the Y-Direction.

Lastly, shown in **Figure 24**, the z-directional trend gave similar results to the X-directional trends. The first two natural frequencies before modification were 13Hz and 26Hz, whereas post modifications were 12Hz and 26Hz. This test only yielded two natural frequencies for post modifications.

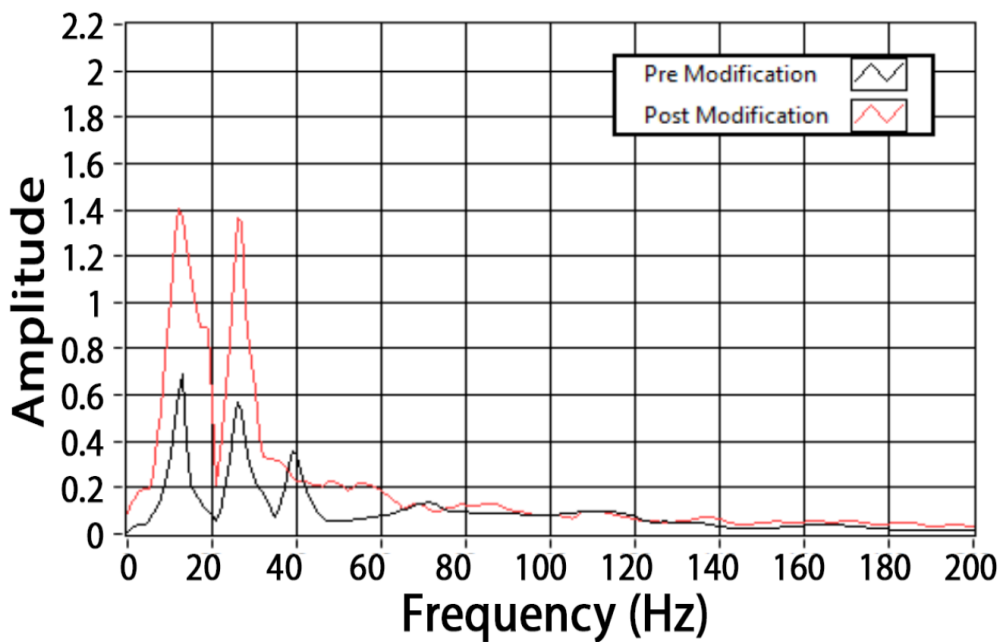


Figure 24: Frequency Responses in the Z-Direction.

When the magnitudes of the first two natural frequencies are compared pre and post modification they show an increase in the frequencies post modification. The first frequency for both before and after modification was 14Hz; however, the second frequency before modifications was 32Hz, and the frequency post modification was 30Hz. This corroborates data from simulations.

3.5.2 Comparing the Magnitude of the First Natural Frequency of the Modified Positioner

The first natural frequency of each method used was determined and compared to ensure the validity of each method. Since all the values are within acceptable ranges of one another, the testing was deemed valid and can be used in the future for further modifications and frequency shifting of the positioner. The results of this comparison are shown in **Table 6**.

Table 6: The Magnitude of the First Natural Frequency of the Modified Positioner Found Analytically, Computationally, and Experimentally.

Analytical	Computational	Experimental
11 Hz	16 Hz	14 Hz

3.5.3 Determining How Each DOF Impacts Stability of Optical Measurements

Holographic testing was performed to determine the effect of each degree of freedom on the stability of optical measurements. The setup for holographic testing is shown in **Figure 25**. In this figure, the optical head is aimed at sample supported by the positioning system. The positioner was moved along three of its course degrees of freedom (Y-translation, pitch, and X-translation) and tested at nine critical locations with testing conditions shown in **Appendix 6**. For each critical location, the rotor was excited to its resonant frequencies within the audible range (20-20,000Hz) and fringes were observed. Fringes are a visual measurement of five torsional and bending mode shapes. Each resonant frequency results in a different mode shape. Stable fringes indicate a stable positioner, whereas unstable (moving) fringes indicate an unstable positioner.

The fringes of certain fan blades were observed at each resonant frequency to measure the stability of the positioner at each critical location.

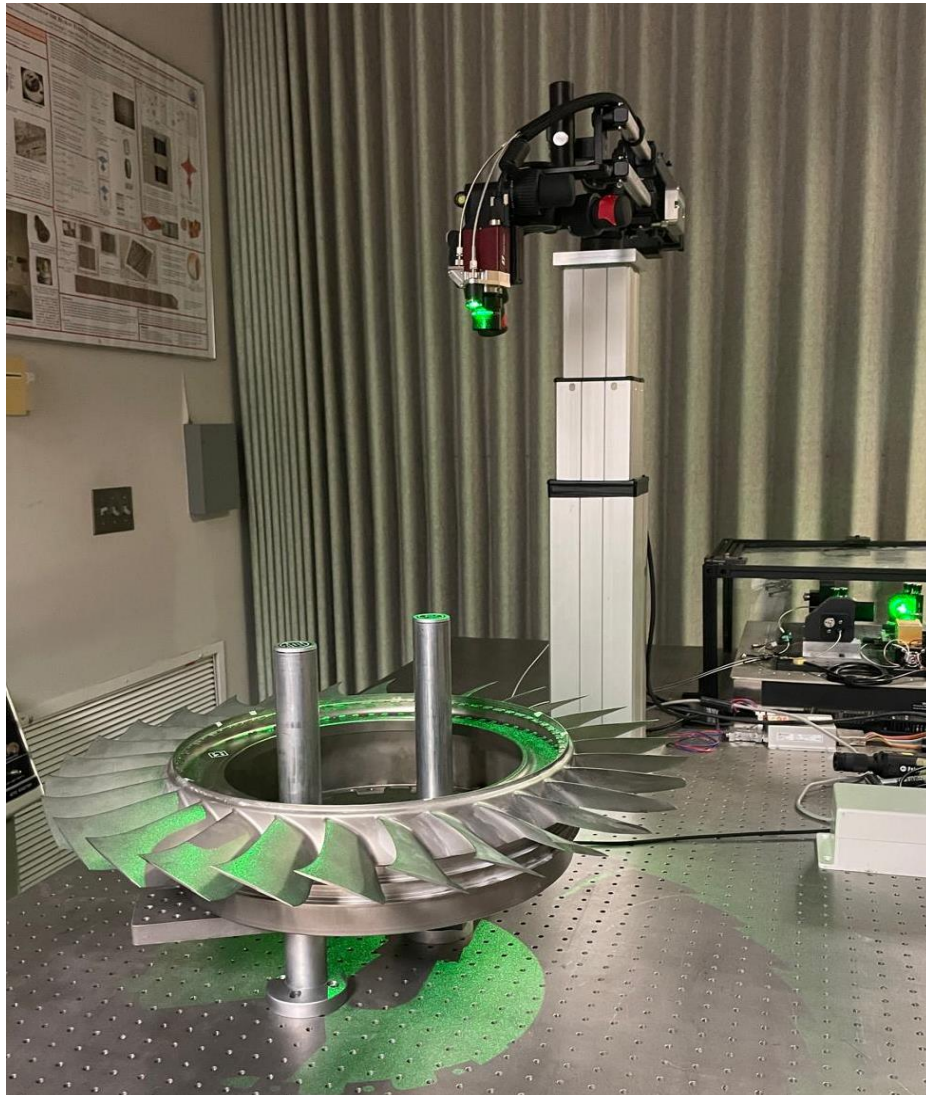


Figure 25: The Setup for Holographic Testing a Representative Rotor Sample.

This test was performed before and after modifications and the results are shown in **Table 7**. The unmodified positioner was unstable while the vertical stand was extended halfway at seventeen centimeters and completely at thirty-two centimeters. The modified positioner was stable at all critical locations, showing a significant increase in stability. The degree of freedom that impacted stability the most was the X-translation of the stand. Additionally, the test stand was less stable at lower frequencies since the positioning system had a large portion of natural

frequencies in the lower range. These findings are critical since the stability of the system determined whether the system could be a deliverable prototype to the sponsor of the project.

Table 7: Fringe Stability for the Unmodified and Modified Positioner.

Positioner Orientation	Fringe Stability for Unmodified Positioner	Fringe Stability for Modified Positioner
Positioner Orientation	Stable	Stable
27cm JIB Extension	Stable	Stable
20cm JIB Extension	Stable	Stable
13cm JIB Extension	Stable	Stable
45 Deg JIB Pitch	Stable	Stable
22.5 Deg JIB Pitch	Stable	Stable
-22.5 Deg JIB Pitch	Stable	Stable
-45 Deg JIB Pitch	Stable	Stable
32 cm Polytec Stand Extension	Unstable	Stable
17 cm Polytec Stand Extension	Unstable	Stable
2 cm Polytec Stand Extension	Stable	Stable

4.0 Results and Applications

Using the realized positioning system, the holographic head was maneuvered around a representative rotor sample positioned horizontally on the optical table to capture holographic images at different locations. The rotor was excited to one of its resonant frequencies using a piezoelectric shaker. Ten holographic images were captured, and the result was stitched together by aligning pixels using Adobe Photoshop. Four individual images and the stitched image of the entire rotor sample are shown below in **Figure 26**. This demonstrates a viable new inspection capability of maneuvering a positioner around a stationary sample while maintaining nanometer resolution to acquire a full scan. This system can be used by the sponsor of the project to expedite holographic testing to ensure the safety of rotors and other aerostructures before their deployment and use.

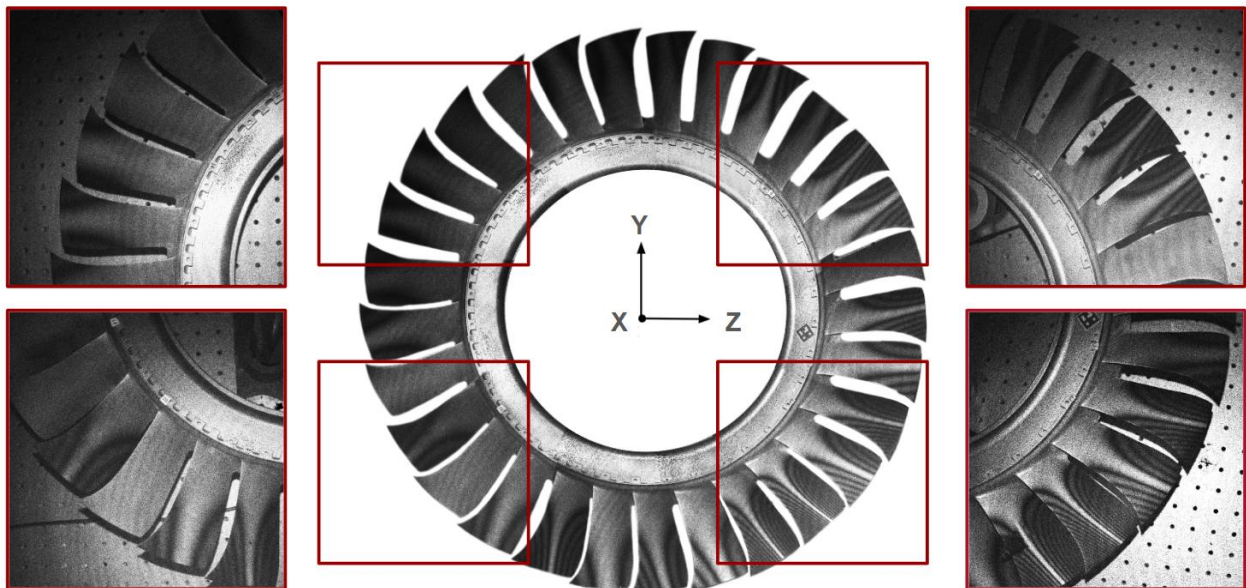


Figure 26: Stitched Holographic Image of a Commercial Avionics Rotor and Four Selected Individual Holographic Images.

5.0 Conclusions and Future Work

This project has successfully delivered a prototype that could be used in the sponsor's facilities to holographically evaluate a rotor blade. Additionally, this project created a testing setup and procedure for testing other types of positioning systems and evaluating them for stability.

The continuation of this project would be additional tuning of the positioning system, as well as further increasing stability, mobility, and user-friendliness. While the system that is currently established works, there is a significant amount of user input required to shift the positioning system to each location. With additional modifications, it can be made more convenient for the user, as well as have increased mobility. Once these modifications are complete, the positioner will have to be tuned again to ensure the system's natural frequencies do not match the natural frequencies of the samples it is testing. Additionally, with each iteration of modifications, it will need to be retested for stability.

Other recommendations would be to utilize engineering software assisted with artificial intelligence to increase the efficiency of computations. Computations take a significant amount of time to complete, as well as much of a computer's processing power. The ability to use software that can complete a significant number of computations in a short time would allow the analysis of a larger number of simulations and therefore, more modifications could be made in a shorter time frame.

References

1. Ali, Z., Sheikh, M. F., Al Rashid, A., Arif, Z. U., Khalid, M. Y., Umer, R., & Koç, M. (2023). Design and development of a low-cost 5-DOF robotic arm for lightweight material handling and sorting applications: A case study for small manufacturing industries of Pakistan. *Results in Engineering*, 19, 101315.
<https://doi.org/10.1016/j.rineng.2023.101315>
2. Aust, J., & Pons, D. (2019). Taxonomy of Gas Turbine Blade Defects. *Aerospace*, 6.
3. Boeing 747SP-J6—Pratt & Whitney | Aviation Photo #6170361 | Airliners.net. (n.d.). Retrieved April 16, 2024
4. Edelkrone JibONE (2024). Maloney Amsterdam. Retrieved April 9, 2024
5. FX Articulating Arm HD 5/8 mount. (2024). Retrieved April 9, 2024
6. Norton, R. L. (2014). *Machine design: An integrated approach* (Fifth edition). Prentice Hall.
7. Pryputniewicz J. Ryszard, (1986) "Quantitative Holographic Analysis Of Small Components," Proc. SPIE 0604, Holographic Nondestructive Testing.
8. Rao, S. (2011). *Mechanical Vibrations* (5th ed.). Pearson Education Inc.
9. Scioscope SB-BM2-S0. (2024). Scioscope Products. Retrieved April 9, 2024
10. Verlag, A. (1996). *Holographic Interferometry* (1st ed.). VCH Publishing Group.

Appendices

Appendix 1: Gantt Chart of A, B, C, and D Term

A Term: Problem Definition and Research									
Milestone	Activity	Week 1 (8/28)	Week 2 (9/4)	Week 3 (9/11)	Week 4 (9/18)	Week 5 (9/25)	Week 6 (10/2)	Week 7 (10/9)	Week 8 (10/16)
Positioner Selection	Research positioners								
	Research principles of holography								
	Determine objectives, functional specifications, and constraints								
	CAD basic positioners								
	Force simulations on basic positioners								
	Modify basic positioners								

B Term: Conceptualization and Idealization									
Milestone	Activity	Week 1 (10/23)	Week 2 (10/30)	Week 3 (11/6)	Week 4 (11/13)	Week 5 (11/20)	Week 6 (11/27)	Week 7 (12/4)	Week 8 (12/11)
Positioner Selection	Determine objectives, functional specs, and constraints								
	Modify basic positioners								
Modeling Positioner	Kinematic model								
	Dynamic model								
	Calculate design parameters								
	Model data from models and calculations								
Attaining Parts	Begin machine design								
	Begin ordering parts								

C Term: Prototyping and Development									
Milestone	Activity	Week 1 (1/10-14)	Week 2 (1/15-21)	Week 3 (1/22-28)	Week 4 (1/29-2/4)	Week 5 (2/5-2/11)	Week 6 (2/12-2/18)	Week 7 (2/19-2/25)	Week 8 (2/26-3/1)
Detailed Design	Reverse engineer the JIB								
	Design additional parts								
	Design backup plan								
	Refine design								
Purchasing components	Order additional parts								
Assembly	Recieve/assemble parts								
Preliminary Testing	LDV activity on JIB								
	Compare resonance frequencies of JIB to rotor								
	Holography activity								
Documentation	report/presentation								

D Term: Testing and Evaluation								
Milestone	Activity	Week 1 (3/11-3/17)	Week 2 (3/18-3/24)	Week 3 (3/25-3/31)	Week 4 (4/1-4/7)	Week 5 (4/8-14)	Week 6 (4/15-4/21)	Week 7 (4/22-4.28)
Detailed Design	Design backup plan							
	Refine design							
Assembly	Machine/assemble components							
Advanced Testing	LDV activity on JIB with replaced parts							
	Holography activity							
	Compare resonance frequencies of new JIB to rotor							
	Stitching activity							
Documentation	Report/presentation							

Appendix 2: Constraints and Functional Specifications

Constraints					
Category	Part	Description	Constraints	Level of Importance (1=most important, 5=least important)	Reasoning
Operation	Optical Head	Working Distance	- lenses changed depending on distances	2	DOF limited by working distance
Safety	Joints	Connections	- Must not be able to harm operator	1	Must be safe
Safety	Optical Head	Optical Fibers	- Must Protect Optical fibers, they are delicate	1	Optical fibers are expensive to replace
Safety	Entire Assembly	Movement	- When positioner is moved, must be safe for technician and protect the machine - All moving parts have to be protected so no appendages get caught	1	Essential for ensuring safe operation
Safety	Entire Assembly	Storage	- Needs to be stable even when disengaged to minimize damage during storage	1	Essential for ensuring safe operation
Cost	Budget	Budget	Must fit within the budget of entire Pratt & Whitney order	4	Set budget
Structure	Cantilever Positioner	Height	- The cantilever structures travel distance will be at the lowest, 490mm and the highest 670mm. This is based on the measurements of the Polytec positioner - This will be designated the x direction	1	In Polytec Stand
Structure	Cantilever Positioner	Width	- 128mm	1	In Polytec Stand
Structure	Cantilever Positioner	Length	- 128mm	1	In Polytec Stand
Structure	Cantilever Positioner	Material	- Aluminum	1	In Polytec Stand
Structure	Cantilever Positioner	Weight Limit	-10kg (22lbs)	1	Property of the Polytec Stand
Structure	Z Directional Arm	Stability	- Must be able to hold the imager and must not vibrate at the same excitation frequencies as the rotor	1	Requirement of P&W
Structure	Wires	Minimum bend radius	Bend radius set by metal layer over cables	1	Cables expensive to replace

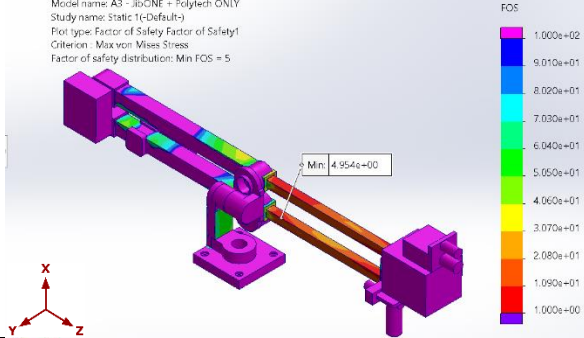
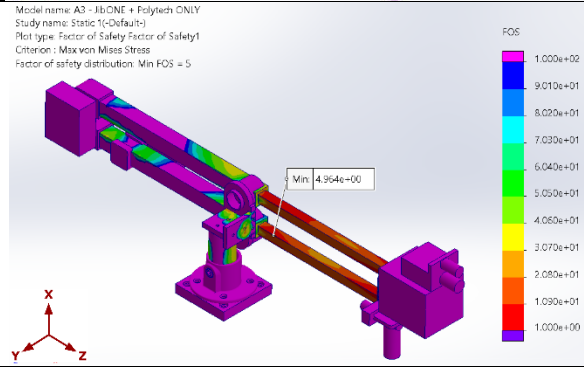
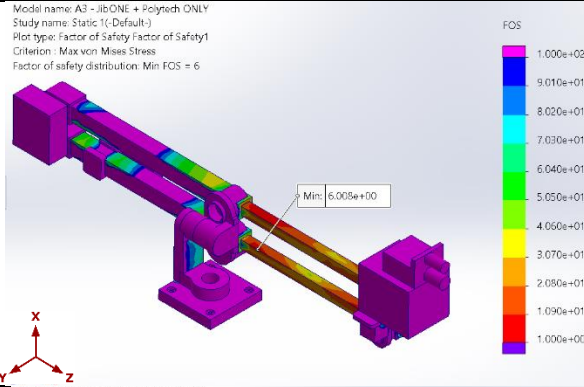
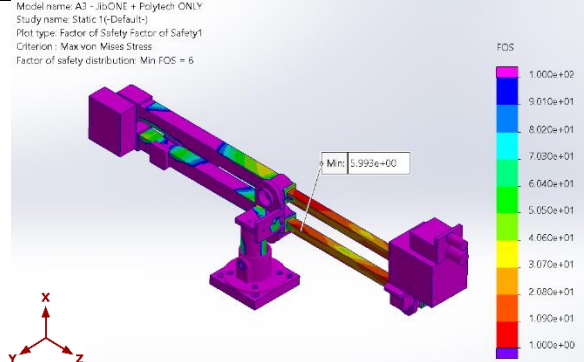
		for electrical and other cable			
Structure	Optical Head	Size	- 60.6(w)x62.2(h)x162.3(l)	3	Positioner must hold optical head
Structure	Optical Table	Size	- 3mx1.5m	1	Optical table is set
Structure	Entire Assembly	Stability	- Positioner must have maximum stability	1	Optics wont work unstable
Structure	Entire Assembly	Cable Management	- Cables will be ≥ 2 m (connecting laser delivery and optical head) - Cables must not be pinched by the assembly - Minimize number of cables as per stated in safety regulations	1	Cables must be safe
Structure	Shaker	Shaker frequency range	- Most components maximum 24kHz	1	Shaker vibrations are set
Structure	Optical Head	Weight	- 2 lbs	1	Must hold head
Structure	Shaker	Height	- Holds blade ~1ft high	1	Shaker dimensions set
Structure	Rotor Sample	Size	-at least 1 ft	2	Positioner must be able to obtain full scan of sample
Structure	Base	Stability	- Must prevent the system from falling and/or prevent extra vibrations	1	Must be stable
Structure	Cantilever Positioner	Connections	- Top and bottom both use M5 socket head cap screws	3	Re-tapping Possible

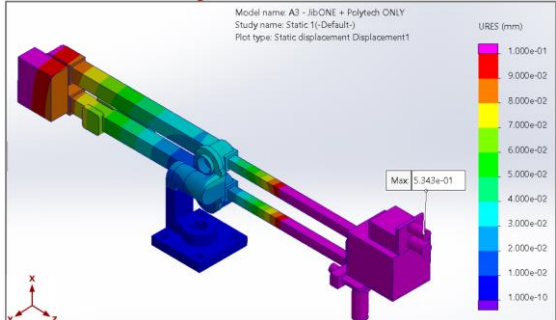
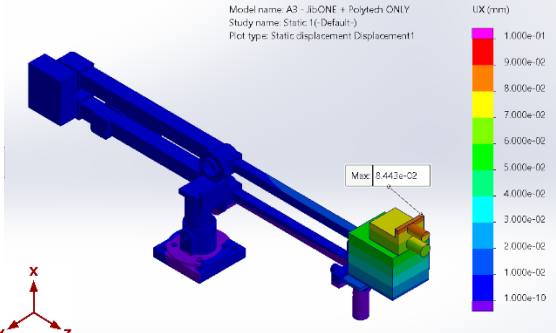
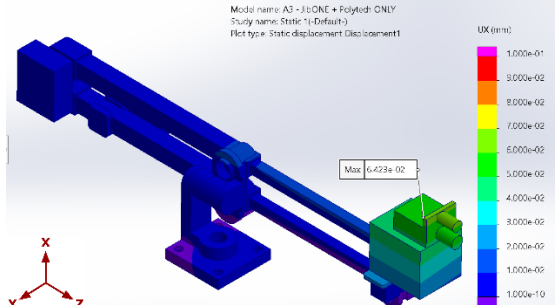
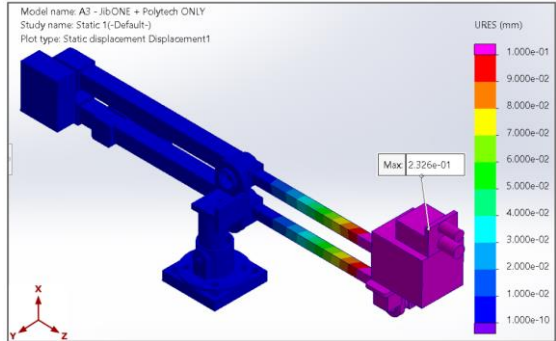
Functional Specifications					
Category	Part	Description	Functional Specification	Level of Importance (1=most important, 5=least important)	Reasoning
Cost	Arm	Purchases	Must fit within the budget of entire Pratt & Whitney order	3	The budget for the entire order is set
Cost	Base	Purchase	Must fit within the budget of entire Pratt & Whitney order	3	The budget for the entire order is set
Cost	Cantilever Positioner	Purchases	Must fit within the budget of entire Pratt & Whitney order	1	The budget for the entire order is set

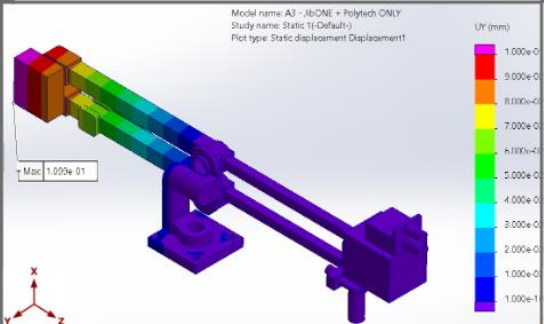
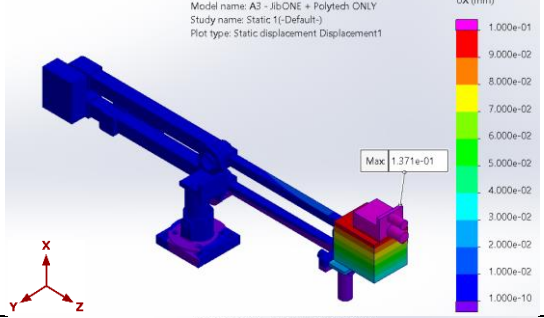
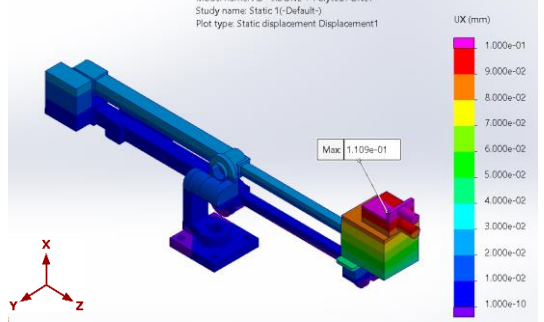
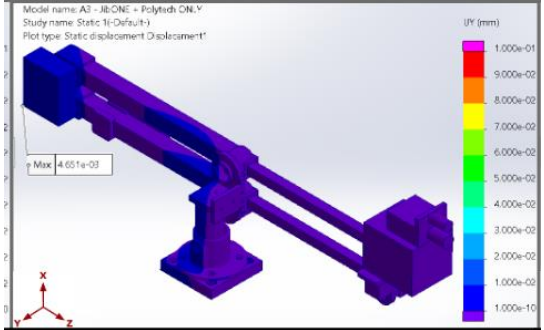
Operation	Base	Movement	- Can be disengaged, moved, and reengaged from the optical table	2	Very important, but possible other ways
Operation	Entire Assembly	Movement	- Moved through options of electrical, hydraulic, pneumatic, and physical - Controlled with Polytec joystick, tie others in	2	Depends on movement methods
Safety	Optical Head	Optical Fibers	- Mount to Frame - Must be flexible enough to move, but stiff enough to stay intact	1	Essential for ensuring safe operation
Safety	Optical Head	Lenses	- Lenses must be handled with care, can not be put into risk by the rest of the assembly	1	Essential for ensuring safe operation
Safety	Entire Assembly	Optical Fibers	- Built with awareness of optical fibers	1	Essential for ensuring safe operation
Structure	Joints	Material	- Aluminum	4	Weight
Structure	Joints	Functionality	- Must be able to be adjusted in the DOF pitch	2	Function ability
Structure	Joints	Connections	- M5 socket head cap screws	3	Already present in stand
Structure	Z Directional Arm	Length	- .5m, with a 3/4 travel length - This will be designated the z direction	3	Length varies
Structure	Z Directional Arm	Thickness	- 60 mm diameter or width - preferably solid material to maximize stability	3	Diameter/thickness varies
Structure	Z Directional Arm	Material	- Aluminum	3	Weight
Structure	Z Directional Arm	Movement	- Must have ability to Pitch and yaw at the end that holds the optical head	2	Important for DOF
Structure	Base	Securing	- Magnetic	3	Can be secured other ways
Structure	Base	Holding Force	- 200 lbs (estimate)	3	Base can be changed

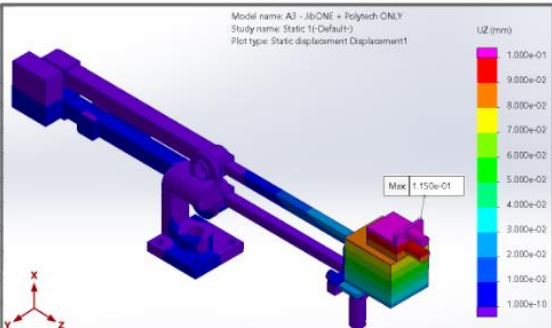
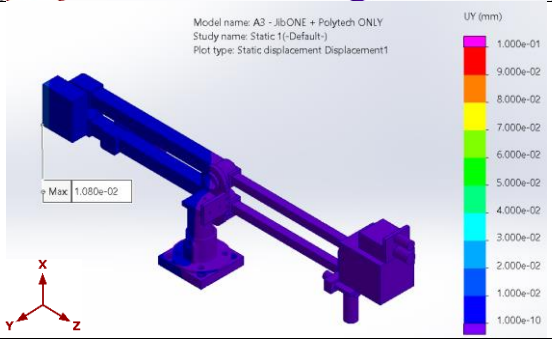
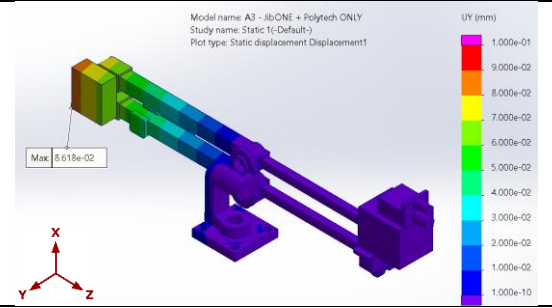
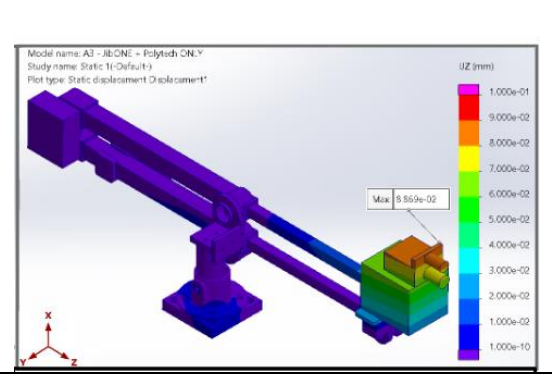
Structure	Base	Size	Must be slightly larger than base of Polytec stand, circular or square	3	Base can be changed
Structure	Joints in arm	Material	- Aluminum	4	Weight
Structure	Positioner DOF	Position of camera range in X direction	- 6 DOF, might change based on rotor size	1	Necessary DOF needs to be determined

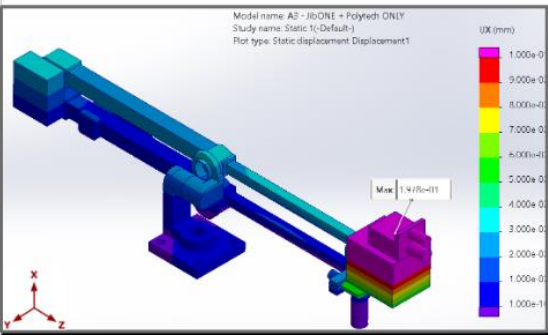
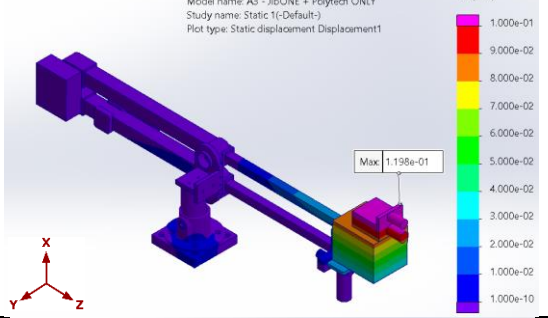
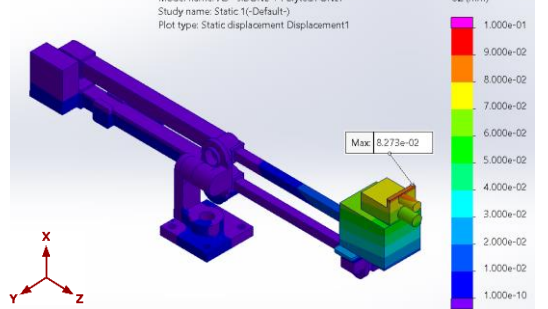
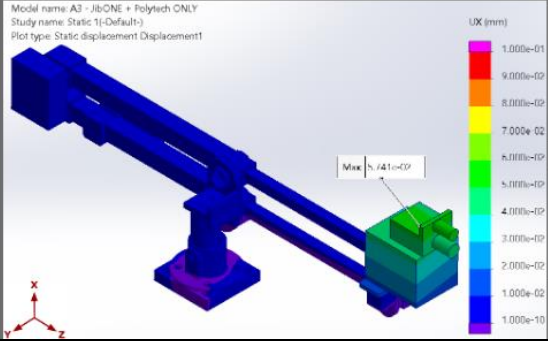
Appendix 3: Static Analysis of Unmodified and Modified Positioner Mechanisms

Modifications to Mechanism	Factor of Safety
<p style="text-align: center;">Unmodified</p>	<p>Model name: A3 - JibONE + Polytech ONLY Study name: Static 1(Default) Plot type: Factor of Safety Factor of Safety1 Criterion: Max von Mises Stress Factor of safety distribution: Min FOS = 5</p> 
<p style="text-align: center;">Modified Base</p>	<p>Model name: A3 - JibONE + Polytech ONLY Study name: Static 1(Default) Plot type: Factor of Safety Factor of Safety1 Criterion: Max von Mises Stress Factor of safety distribution: Min FOS = 5</p> 
<p style="text-align: center;">Modified End Effector</p>	<p>Model name: A3 - JibONE + Polytech ONLY Study name: Static 1(Default) Plot type: Factor of Safety Factor of Safety1 Criterion: Max von Mises Stress Factor of safety distribution: Min FOS = 6</p> 
<p style="text-align: center;">Modified Base and End Effector</p>	<p>Model name: A3 - JibONE + Polytech ONLY Study name: Static 1(Default) Plot type: Factor of Safety Factor of Safety1 Criterion: Max von Mises Stress Factor of safety distribution: Min FOS = 6</p> 

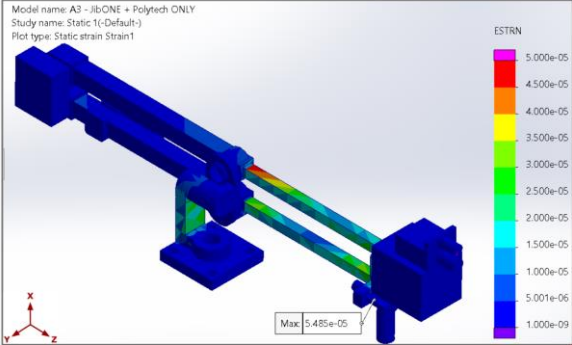
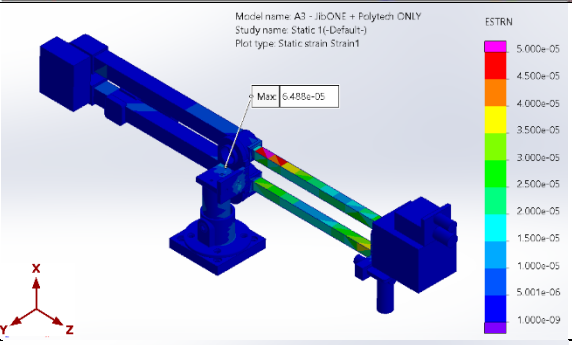
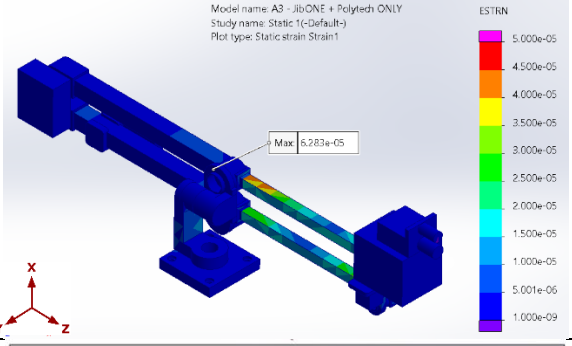
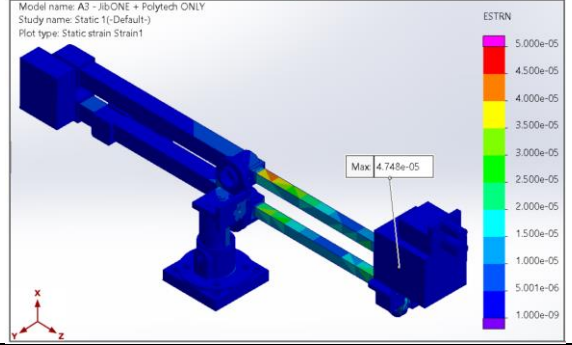
Modifications to Mechanism	Resultant Displacement (mm)
<p align="center">Unmodified</p>	 <p>Model name: A3 - JibONE + Polytech ONLY Study name: Static 1(-Default-) Plot type: Static displacement Displacement1</p> <p>URES (mm)</p> <p>Max: 5.343e-01</p>
<p align="center">Modified Base</p>	 <p>Model name: A3 - JibONE + Polytech ONLY Study name: Static 1(-Default-) Plot type: Static displacement Displacement1</p> <p>UX (mm)</p> <p>Max: 8.443e-02</p>
<p align="center">Modified End Effector</p>	 <p>Model name: A3 - JibONE + Polytech ONLY Study name: Static 1(-Default-) Plot type: Static displacement Displacement1</p> <p>UX (mm)</p> <p>Max: 6.423e-02</p>
<p align="center">Modified Base and End Effector</p>	 <p>Model name: A3 - JibONE + Polytech ONLY Study name: Static 1(-Default-) Plot type: Static displacement Displacement1</p> <p>URES (mm)</p> <p>Max: 2.326e-01</p>

Modifications to Mechanism	Displacement in X-Direction (mm)
Unmodified	 <p>Model name: A3 - JibONE + Polytech ONLY Study name: Static 1(Default) Plot type: Static displacement Displacement1</p> <p>UX (mm)</p> <p>Max: 1.050e-01</p>
Modified Base	 <p>Model name: A3 - JibONE + Polytech ONLY Study name: Static 1(Default) Plot type: Static displacement Displacement1</p> <p>UX (mm)</p> <p>Max: 1.371e-01</p>
Modified End Effector	 <p>Model name: A3 - JibONE + Polytech ONLY Study name: Static 1(Default) Plot type: Static displacement Displacement1</p> <p>UX (mm)</p> <p>Max: 1.109e-01</p>
Modified Base and End Effector	 <p>Model name: A3 - JibONE + Polytech ONLY Study name: Static 1(Default) Plot type: Static displacement Displacement1</p> <p>UX (mm)</p> <p>Max: 4.651e-03</p>

Modifications to Mechanism	Displacement in Y-Direction (mm)
<p>Unmodified</p>	 <p>Model name: A3 - JibCONE + Polytech ONLY Study name: Static 1(-Default) Plot type: Static displacement Displacement1</p> <p>UZ (mm)</p> <p>Max 1.150e-01</p>
<p>Modified Base</p>	 <p>Model name: A3 - JibCONE + Polytech ONLY Study name: Static 1(-Default) Plot type: Static displacement Displacement1</p> <p>UY (mm)</p> <p>Max 1.080e-02</p>
<p>Modified End Effector</p>	 <p>Model name: A3 - JibCONE + Polytech ONLY Study name: Static 1(-Default) Plot type: Static displacement Displacement1</p> <p>UY (mm)</p> <p>Max 5.618e-02</p>
<p>Modified Base and End Effector</p>	 <p>Model name: A3 - JibCONE + Polytech ONLY Study name: Static 1(-Default) Plot type: Static displacement Displacement1</p> <p>UZ (mm)</p> <p>Max 8.859e-02</p>

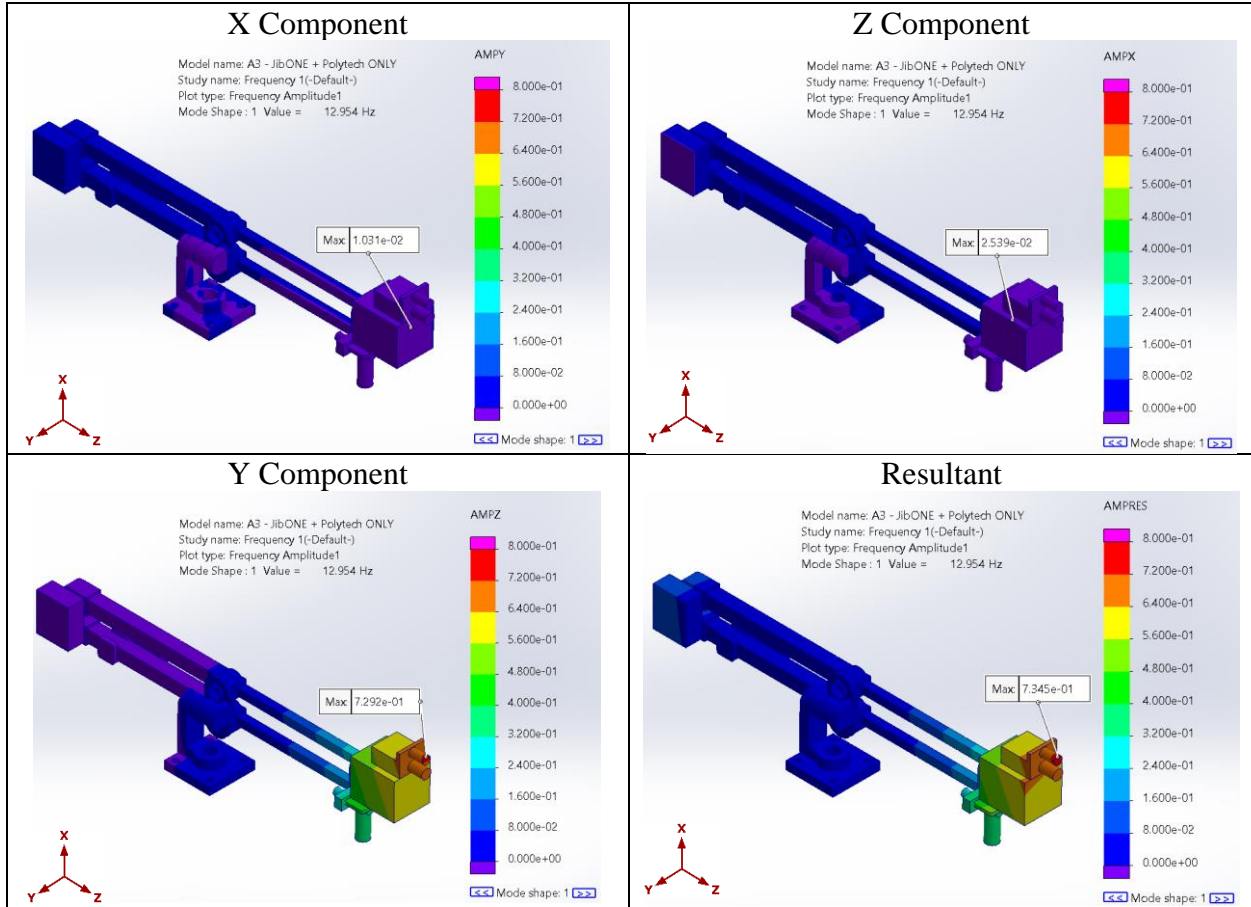
Modifications to Mechanism	Displacement in Z-Direction (mm)
<p style="text-align: center;">Unmodified</p>	 <p>Model name: A3 - JibONE + Polytech ONLY Study name: Static 1(-Default-) Plot type: Static displacement Displacement1</p> <p>Max: 1.4776e-11</p> <p>UZ (mm)</p>
<p style="text-align: center;">Modified Base</p>	 <p>Model name: A3 - JibONE + Polytech ONLY Study name: Static 1(-Default-) Plot type: Static displacement Displacement1</p> <p>Max: 1.198e-01</p> <p>UZ (mm)</p>
<p style="text-align: center;">Modified End Effector</p>	 <p>Model name: A3 - JibONE + Polytech ONLY Study name: Static 1(-Default-) Plot type: Static displacement Displacement1</p> <p>Max: 8.273e-02</p> <p>UZ (mm)</p>
<p style="text-align: center;">Modified Base and End Effector</p>	 <p>Model name: A3 - JibONE + Polytech ONLY Study name: Static 1(-Default-) Plot type: Static displacement Displacement1</p> <p>Max: 5.141e-02</p> <p>UZ (mm)</p>

Modifications to Mechanism	Von Mises Stress (N/m ²)
Unmodified	<p>Model name: A3 - JibONE + Polytech ONLY Study name: Static 1(-Default-) Plot type: Static nodal stress Stress1</p> <p>von Mises (N/m²)</p> <p>Max: 6.893e+06</p>
Modified Base	<p>Model name: A3 - JibONE + Polytech ONLY Study name: Static 1(-Default-) Plot type: Static nodal stress Stress1</p> <p>von Mises (N/m²)</p> <p>Max: 3.423e+06</p>
Modified End Effector	<p>Model name: A3 - JibONE + Polytech ONLY Study name: Static 1(-Default-) Plot type: Static nodal stress Stress1</p> <p>von Mises (N/m²)</p> <p>Max: 7.681e+05</p>
Modified Base and End Effector	<p>Model name: A3 - JibONE + Polytech ONLY Study name: Static 1(-Default-) Plot type: Static nodal stress Stress1</p> <p>von Mises (N/m²)</p> <p>Max: 4.585e+06</p>

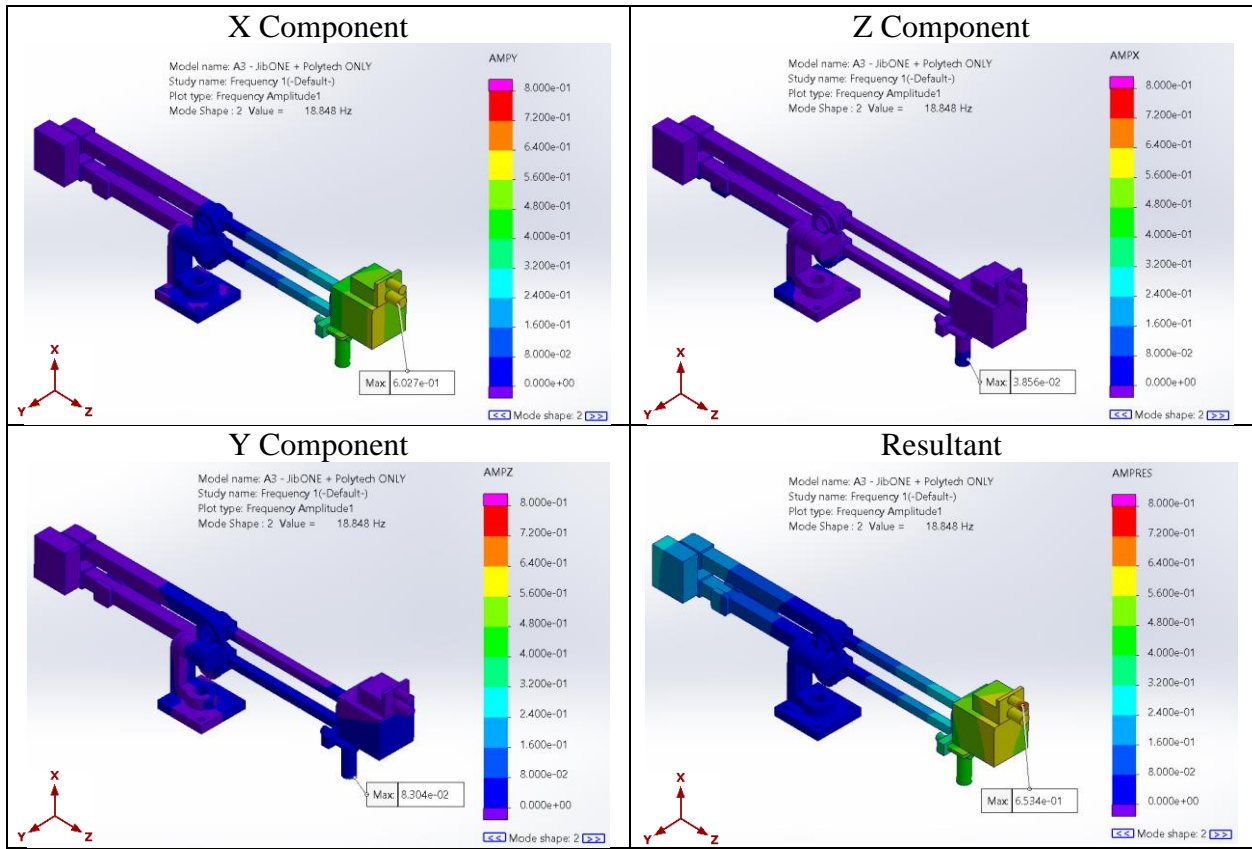
Modifications to Mechanism	Strain
Unmodified	 <p>Model name: A3 - JibONE + Polytech ONLY Study name: Static 1(-Default-) Plot type: Static strain Strain1</p> <p>Max: 5.485e-05</p> <p>ESTRN color scale: 5.000e-05 to 1.000e-09</p>
Modified Base	 <p>Model name: A3 - JibONE + Polytech ONLY Study name: Static 1(-Default-) Plot type: Static strain Strain1</p> <p>Max: 5.495e-05</p> <p>ESTRN color scale: 5.000e-05 to 1.000e-09</p>
Modified End Effector	 <p>Model name: A3 - JibONE + Polytech ONLY Study name: Static 1(-Default-) Plot type: Static strain Strain1</p> <p>Max: 5.283e-05</p> <p>ESTRN color scale: 5.000e-05 to 1.000e-09</p>
Modified Base and End Effector	 <p>Model name: A3 - JibONE + Polytech ONLY Study name: Static 1(-Default-) Plot type: Static strain Strain1</p> <p>Max: 4.748e-05</p> <p>ESTRN color scale: 5.000e-05 to 1.000e-09</p>

Appendix 4: Dynamic Analysis of Unmodified and Modified Positioner Mechanisms

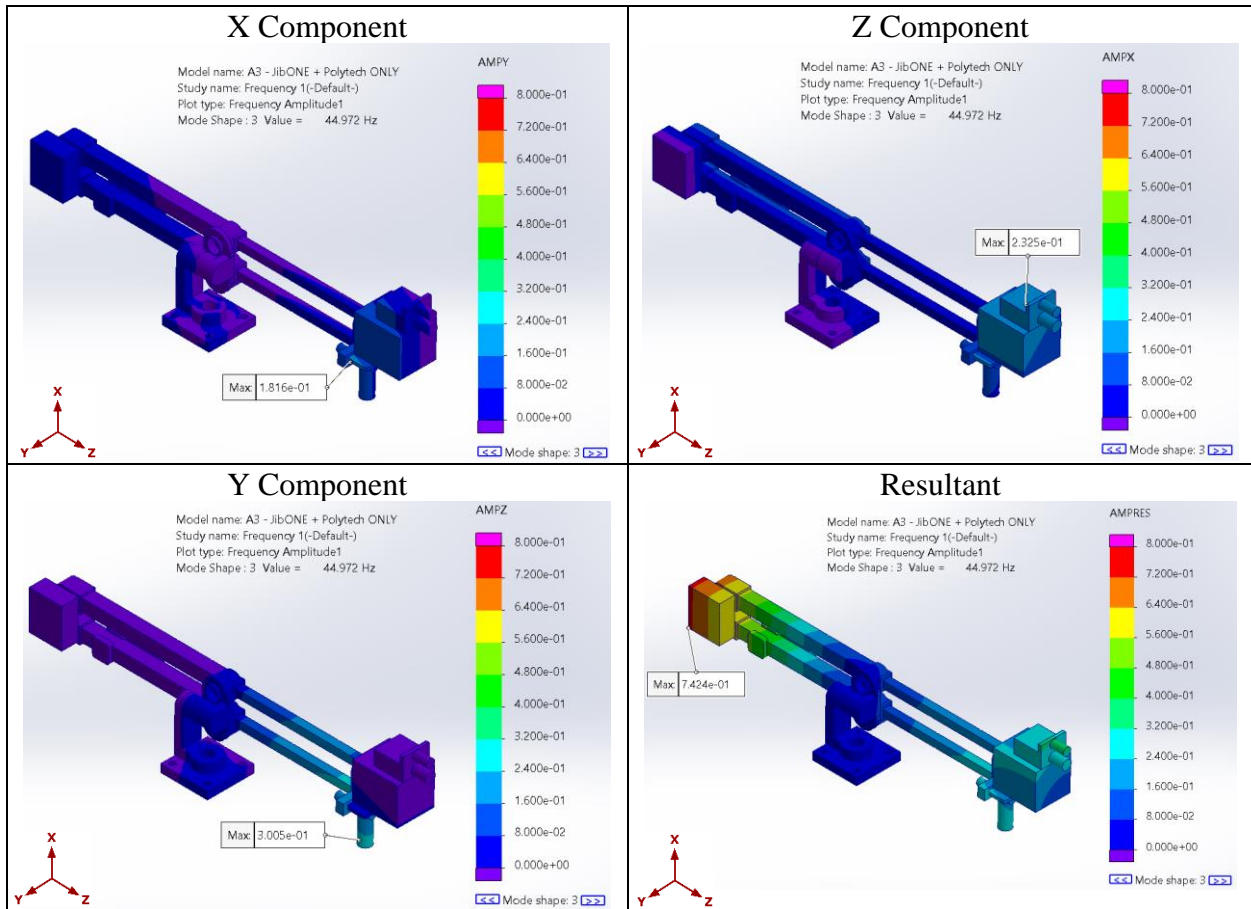
Mode 1 Before Modifications



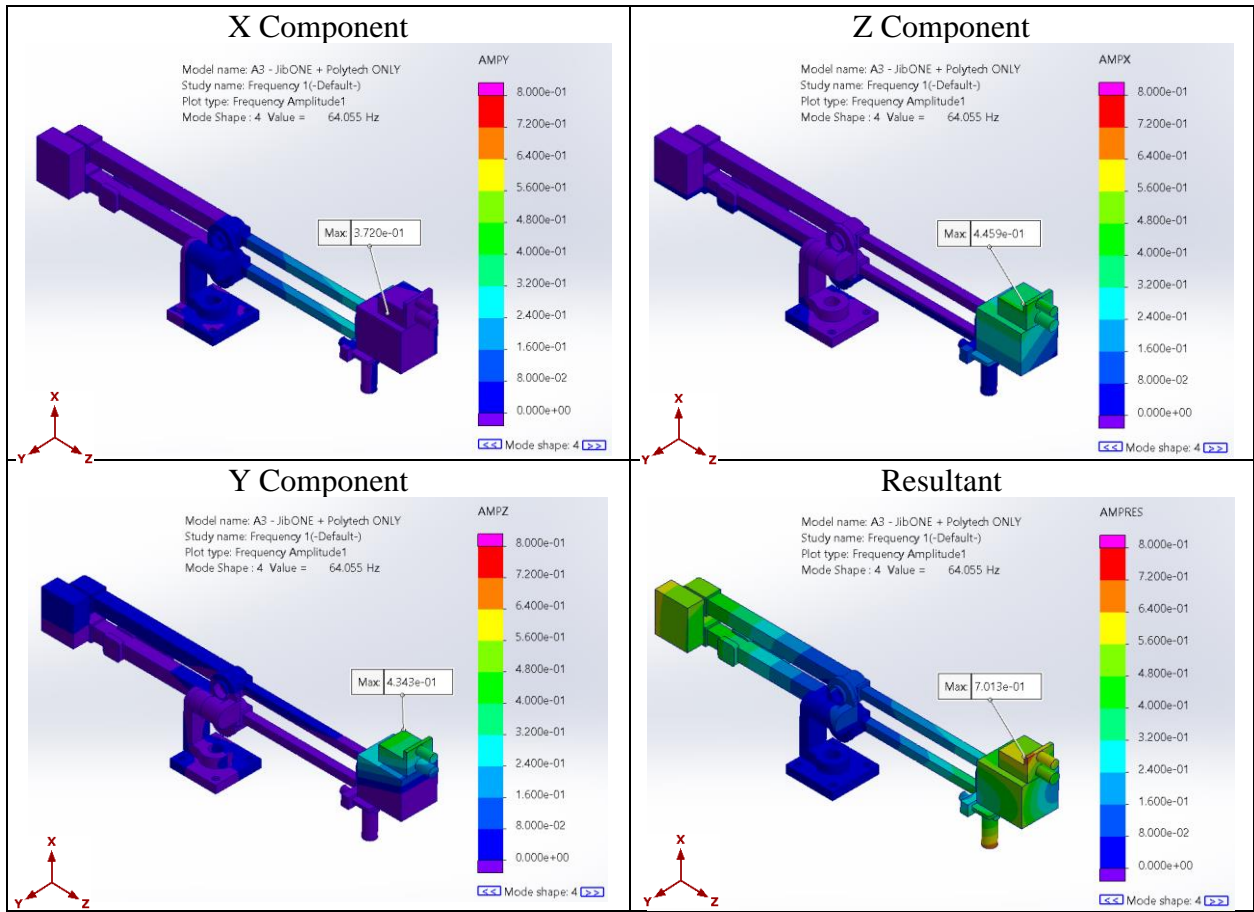
Mode 2 Before Modifications



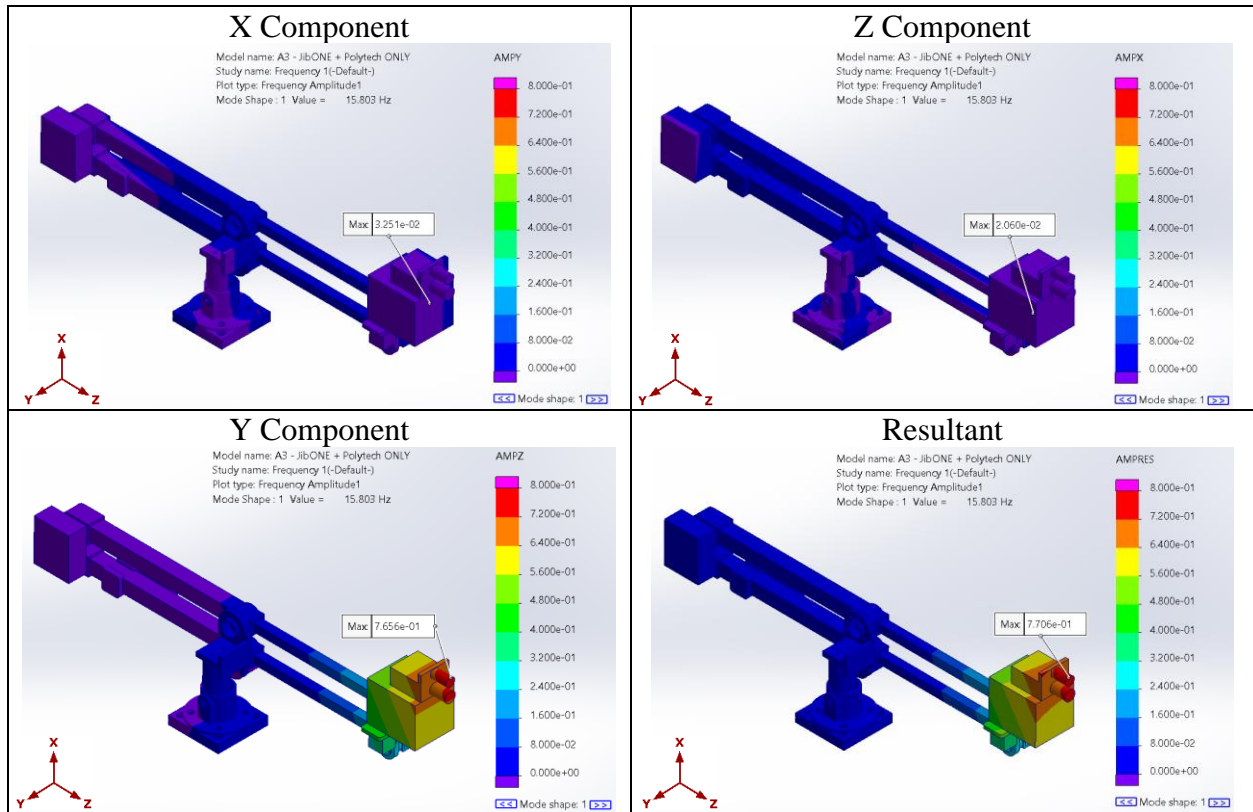
Mode 3 Before Modifications



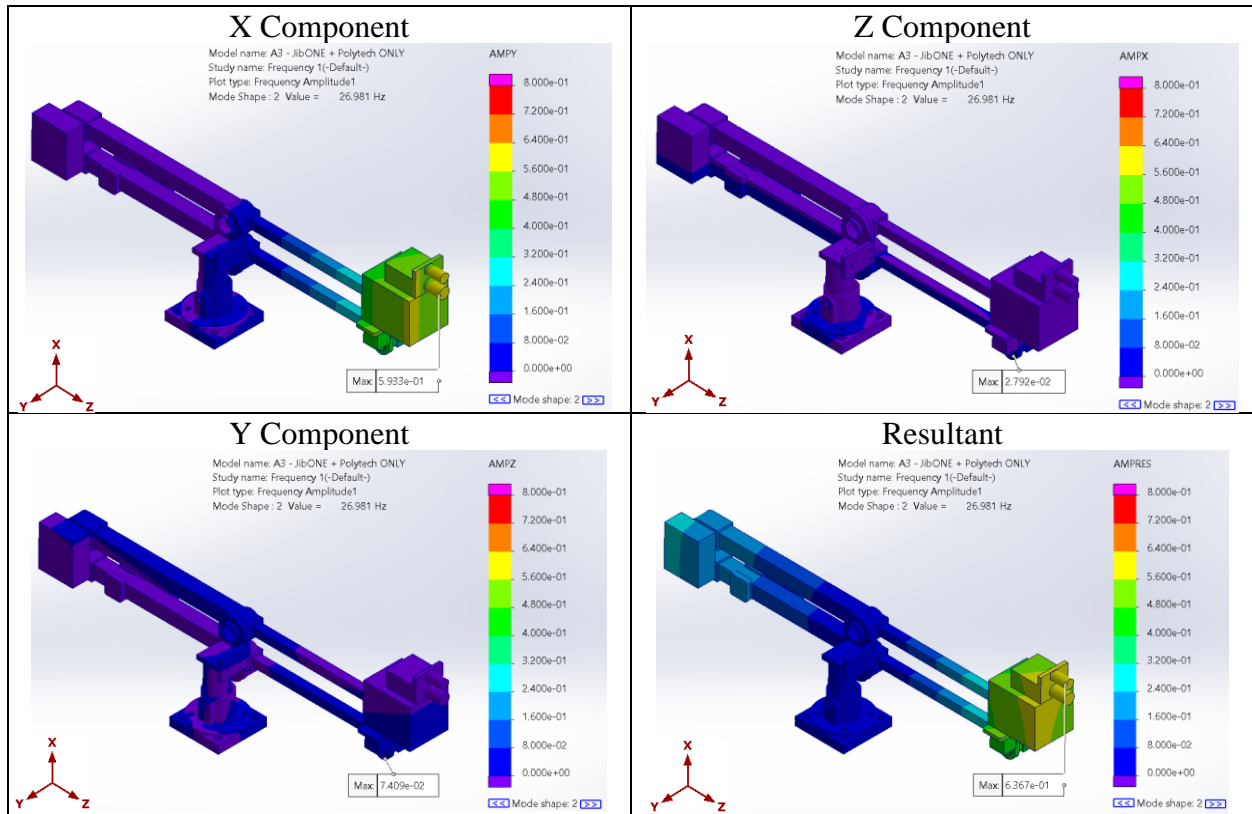
Mode 4 Before Modifications



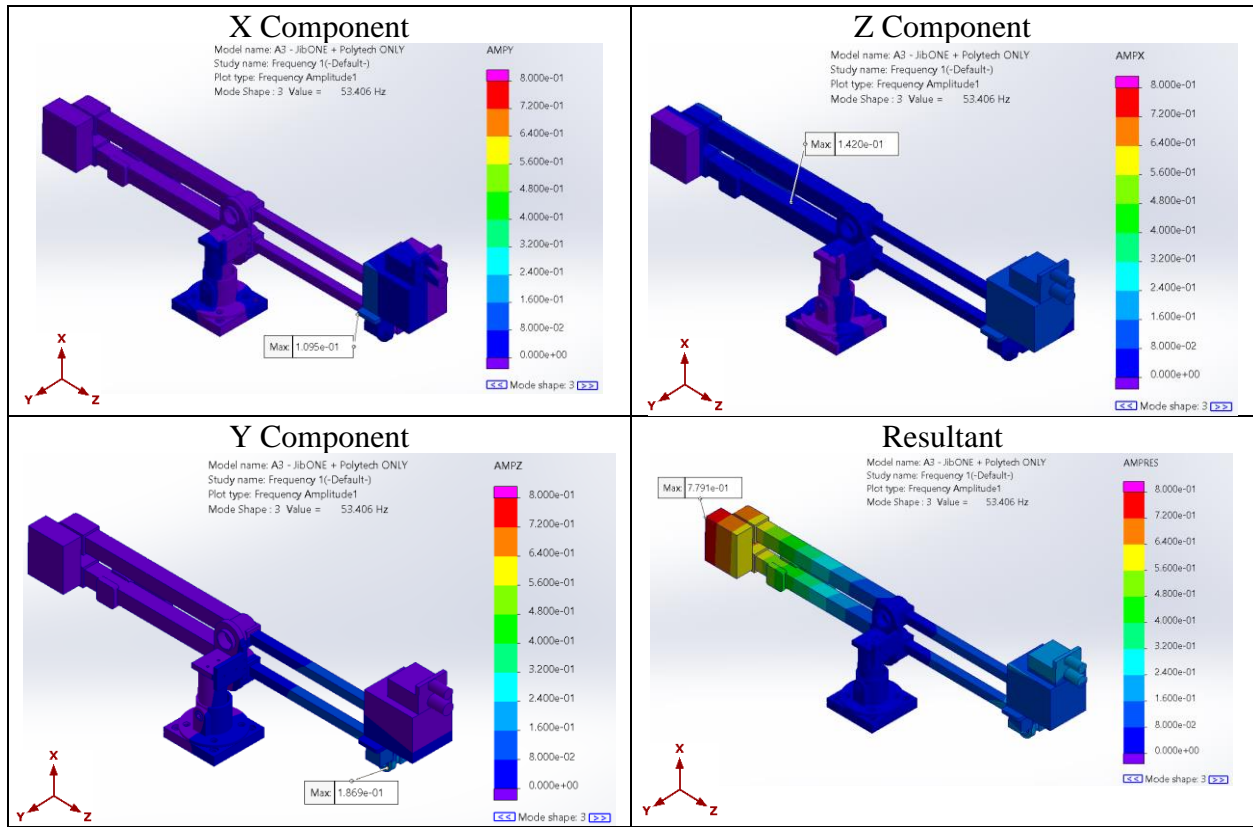
Mode 1 With a Modified Base of the Four bar Mechanism and End Effector



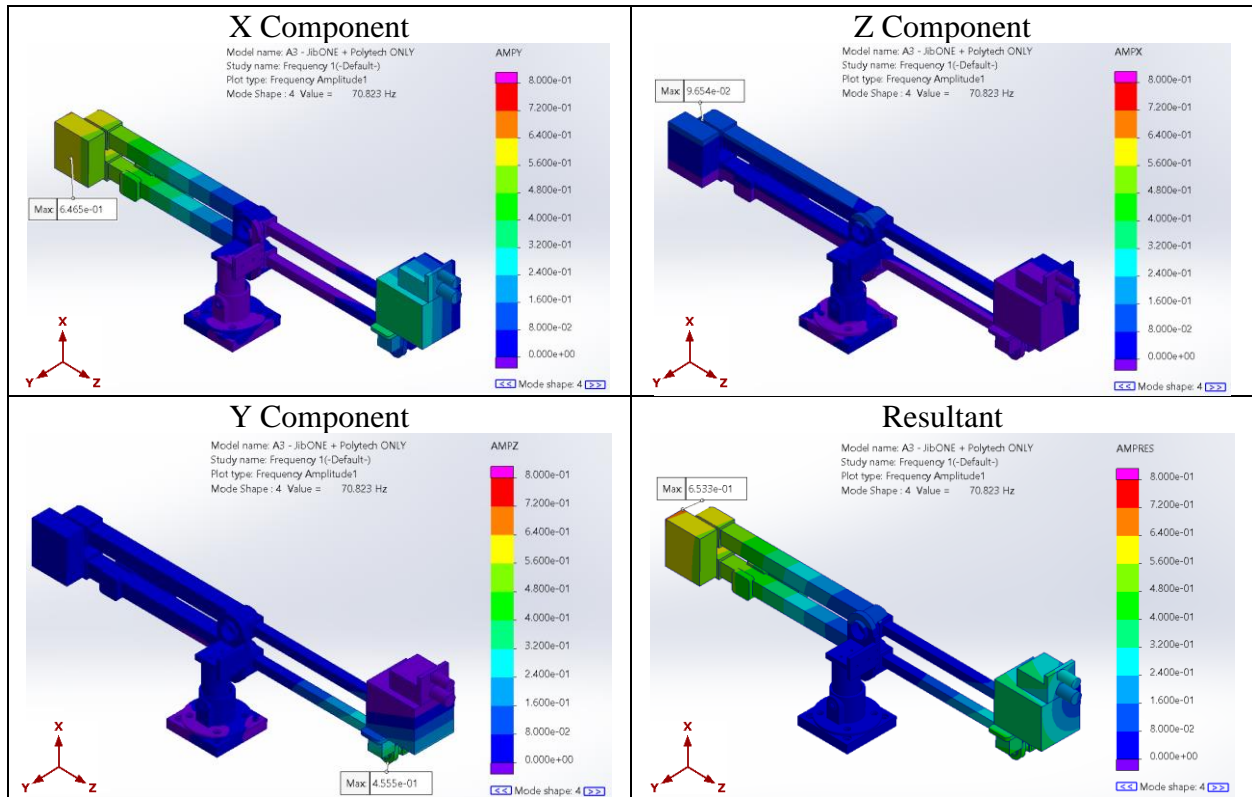
Mode 2 With a Modified Base of the Four bar Mechanism and End Effector



Mode 3 With a Modified Base of the Four bar Mechanism and End Effector

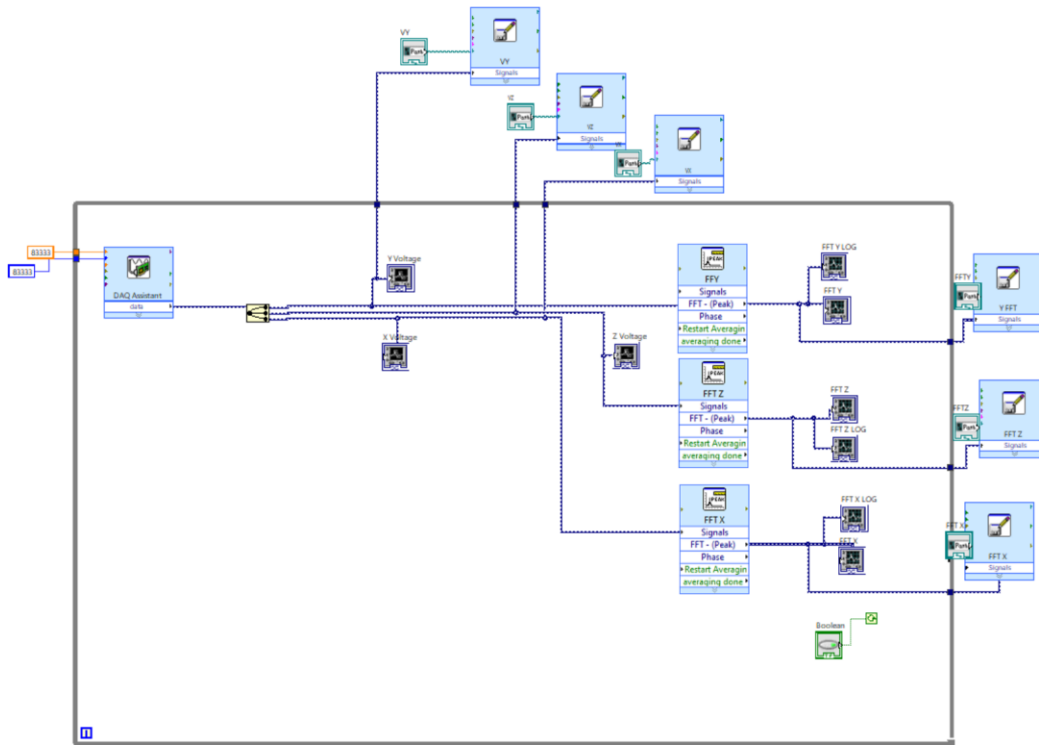


Mode 4 With a Modified Base of the Four bar Mechanism and End Effector



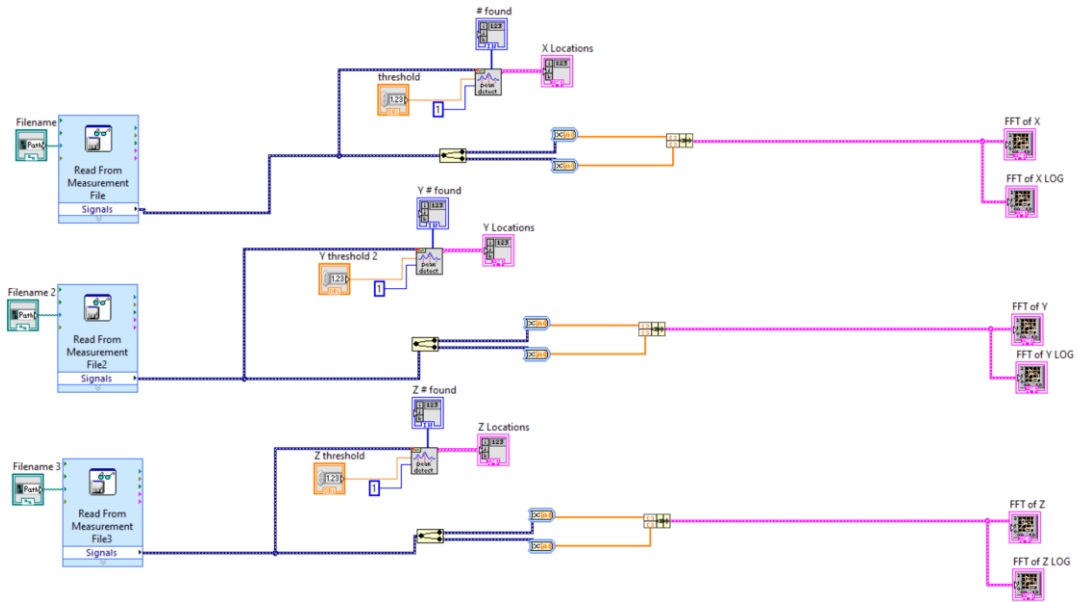
Appendix 5: LabVIEW Programs

Live FFT Analysis



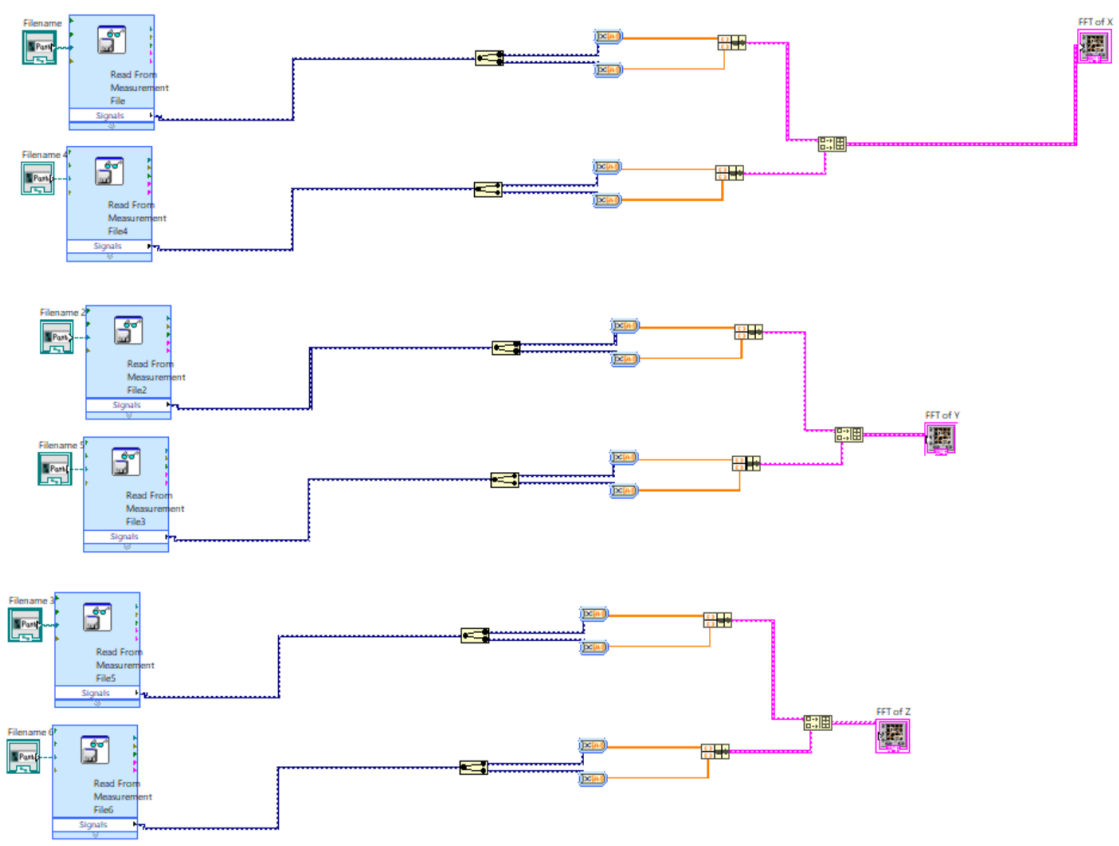
This LabVIEW program started with a DAQ Assistant to acquire the signals from the LDVs. This system was then split into three channels, one for each LDV, and graphed. This was done to ensure the velocity measurements were shown in the program. Following that, Fast Fourier transforms were performed, windowed and averaged, allowing for the determination of individual frequencies. These were then graphed both linearly, and logarithmically along the y axis for visual representation of the data shown over time. The data was saved so it could be edited later. All components of the program with the exception of the data saving were performed in a loop so the program could constantly acquire data and present the information in real time.

Graph Editing



This program reads the saved measurements and splits the data into two different paths. The first path graphs the data. The second path determines the peaks of the data so it they can be easily found, and the thresholds for the peaks can be adjusting depending on the data.

Overlaying Modifications



This program reads the saved for two signals, combines them down to a single array, and graphs it allowing for the comparison of data. This was done specifically in this project to compare pre and post modifications and download graphs of that.

Appendix 6: Test Conditions to Determine How Each DOF Impacts Stability of Optical Measurements

Test Name	Extension of Polytec stand (cm)	Extension of JIB (cm)	Angle of Pitch (degrees)	# of counterweights	Distance of counterbalance to end (cm)	Rotor orientation
Different JIB extensions (Z-translation)	2 (min height)	27	0	1	0	horizontal
	2 (min height)	20	0	1	13	horizontal
	2 (min height)	13	0	0	No counterbalance	horizontal
Different JIB pitches	2 (min height)	27	45	1	0	horizontal
	2 (min height)	27	22.5	1	0	horizontal
	2 (min height)	27	-22.5	1	0	horizontal
	2 (min height)	27	-45	1	0	horizontal
Different Polytec stand heights (X-translation)	32 (max height)	27	0	1	0	horizontal
	17 (1/2 height)	27	0	1	0	horizontal